PCCP
Physical Chemistry Chemical Physics

Accepted Manuscript

This article can be cited before page numbers have been issued, to do this please use: A. Palii, J. M. Clemente Juan, A. Rybakov, S. M. Aldoshin and B. Tsukerblat, *Phys. Chem. Chem. Phys.*, 2021, DOI: 10.1039/D1CP00444A.

Toward multifunctional molecular cells for quantum cellular automata: exploitation of interconnected charge and spin degrees of freedom

View Article Online
DOI: 10.1039/D1CP00444A

Andrew Palii,*[,1] Juan Modesto Clemente-Juan,[2] Andrey Rybakov,[1,3]
Sergey Aldoshin,[1] Boris Tsukerblat*[,4]

[1]*Laboratory of Molecular Magnetic Nanomaterials, Institute of Problems of Chemical Physics, Academician Semenov* avenue *1*, *Chernogolovka, Moscow Region, 142432 Russian Federation*

[2]*Instituto de Ciencia Molecular, Universidad de Valencia, 46980 Paterna, Spain*

[3]*Moscow Institute of Physics and Technology, Institutskii per. 9, Dolgoprudny, Moscow Region, 141701 Russian Federation*

[4]*Department of Chemistry, Ben-Gurion University of the Negev, 84105 Beer-Sheva, Israel*

*E-mail: andrew.palii@uv.es; tsuker@bgu.ac.il

Abstract

We discuss a possibility to use mixed-valence (MV) dimers comprising paramagnetic metal ions as molecular cells for quantum cellular automata (QCA). Thus, we propose to combine the underlying idea behind the functionality of QCA of using the charge distributions to encode binary information with the additional functional options provided by the spin degrees of freedom. The multifunctional ("smart") cell is supposed to consist of multielectron MV $d^n - d^{n+1}$ - type ($1 \leq n \leq 8$) dimers of transition metal ions as building blocks for composing bi-dimeric square planar cells for QCA. The theoretical model of such a cell involves the double exchange (DE), Heisenberg-Dirac-Van Vleck (HDVV) exchange, Coulomb repulsion between the two excess electrons belonging to different dimeric half-cells and also the vibronic coupling. Consideration is focused on the topical case then the difference in Coulomb energies of the two excess electrons occupying nearest neighboring and distant positions significantly exceeds both the electron transfer integral and the vibronic energy. In this case the ground spin-state of the isolated square cell is shown to be the result of competition of the second-order DE producing ferromagnetic effect and the HDVV exchange that is assumed to be antiferromagnetic. In order to reveal the functionality of the magnetic cells, the cell-cell response function is studied within the developed model. The interaction of the working cell with the polarized driver-cell is shown to produce an antiferromagnetic effect tending to suppress the ferromagnetic second-order DE. As a result, under some conditions the electric field of the driver cell is shown to force the working cell to exhibit spin-switching from the state with maximum dimeric spin values to that having minimal spin values.

View Article Online
DOI: 10.1039/D1CP00444A

Abbreviations:

DE -double exchange,

HDVV exchange- Heisenberg-Dirac-Van Vleck exchange

QCA - Quantum Cellular Automata

CMOS - complementary metal–oxide–semiconductor

MV- mixed valence

PKS model- Piepho, Krausz and Schatz model

JT problem- Jahn-Teller problem

1. Introduction

Topical technology based on quantum cellular automata (QCA) has great prospects in competing with the traditional complementary metal–oxide–semiconductor (CMOS) technology in the field of logic elements for digital integrated circuits, and in future is expected to provide a basis for manufacturing of components for electronic devices and computing.[1-4] Being current-free in their nature QCA provide ultra-low heat release as compared with CMOS. Due to this advantage, the QCA devices are of great potential importance to perform computations at very high switching rate.

The cells should satisfy at least two main requirements to requisite successful functioning of QCA devices. First, the "working cells" must be bistable to be able to encode binary information. The two states of the cell arise from the two charge distributions, which encode binary **0** and **1**. These states are degenerate in an isolated cell, but the degeneracy is removed so that one of these configurations becomes the ground state if the cell is allowed to interact with the polarized neighboring "driver-cell". Altering the driver-cell induced electrostatic perturbation one can force the working cell to switch between the two binary states **0** and **1**. The second requirement to the functioning cell which is also of primary importance is that switching between the two configurations should occur in a nonlinear abrupt manner. This means that the molecule (or combination of molecules) acting as molecular cell should be easily polarizable by the external electrostatic perturbation that means that small perturbation should results in a strong reply of the working cell.

The pioneering proposal in the area of QCA has been based on the quantum dot -based cells coupled via Coulomb interaction to form a cellular automata architecture.[1, 5-12] Each such cell typically consists of four quantum dots situated in the vertices of the square and two electrons (or holes) tunneling between these dots. The binary information **0** and **1** is encoded in the two states which correspond to the localizations of the mobile electron at the diagonals of the square. A

contemporary trend in quantum electronics is the development of molecular QCA, which can be regarded as a further step in the miniaturization of QCA based on quantum dots. [13-16] Mixed valence (MV) complexes containing mobile extra electrons have been proposed as natural candidates to act as molecular cells, which would satisfy the requirements of bistability and polarizability. The role of the quantum dots in such molecule is played by the redox sites, which are linked by the bridging ligands mediating the electron tunneling.

As far as the binary information in a molecular cell is encoded in the two charge distributions the stability of these configurations becomes an actual question when we discuss functionality of a cell. A qualitative guide is provided by the well known Robin and Day classification of MV complexes (quantitative discussion will be done in Sections 7 and 8) according to the degree of localization . From the point of view of Robin and Day classification of the strongly delocalized MV complexes belonging to the class III are hardly polarizable by an electric field and so they are not feasible candidates for molecular cells. Also if the MV molecule belongs to strongly localized class I it is getting "stuck" in one polarization and the encoded information cannot be efficiently switched by the field of neighboring molecule. For this reason, the class I systems are not suitable for the use as QCA cells. A compromise choice is to use the systems exhibiting moderate electronic delocalization belonging to the class II or at the borderline between classes II and III. Therefore, the problem of the rational design of the cells based on MV molecules is of crucial importance for the area of molecular QCA. [16-34]

The two possible ways for the design of the molecule based square cells with two mobile charges have been proposed [14], and the comparative analysis of the functional characteristics of cells obtained in these two ways have been done.[35,36] One way is to use two identical MV dimers (referred to as "half-cells") to compose the square cell. An alternative way is to consider a tetranuclear MV cluster comprising two mobile electrons as a ready square cell. Bearing in mind these two possibilities, several MV complexes have been proposed as candidates for molecular implementation of dimeric half cells [16, 18-20, 23, 28] and ready tetrameric square cells. [24-27, 29,30] Still, the search of MV complexes satisfying the above stated criteria represents a very difficult task, and so the number of reported such kind systems remains relatively scarce, although a significant progress in the design of molecular cells for QCA has been achieved during the last yeas.[28, 32] It is to be noted that up to now all reported MV molecules suitable for the design of cells belong to the class of systems in which the extra charges (electrons or holes) are delocalized over the network of diamagnetic sites such as diamagnetic ions in metal complexes or diamagnetic quantum dots.

Recently [37,38] we have proposed to expand the scope of potential molecular cells by including systems in which excess electrons can jump among paramagnetic "spin cores". The cells of this type can be composed of paramagnetic multielectron quantum dots [39-41] or can represent MV

molecules with similar properties [42-49]. This expansion of the range of the relevant systems would not only allow involve a larger number of molecules but also (and probably what is more important) to explore new expected physical features of these systems. Just this aspect will be in the focus of the study in the article. The main physical feature that can be implied by the magnetic ions is a spin polarization caused by the mobile electrons that is known as double exchange (DE) [50-53] and makes such system promising for molecular electronics and spintronics. [54-56]. In recent years significant progress has been achieved in the quantitative evaluation of the effect of the DE with the aid of advanced quantum-chemical methods (see [57] and refs. therein).

In the short communication [37] we have presented preliminary and particular results focused on the isolated and interacting square cells composed of MV $d^n - d^{n+1}$- dimers exhibiting DE and HDVV exchange. For the illustrative purposes it has been assumed that the transfer parameter t describing the one-electron jumps in each dimeric half-cell is much smaller than the gap U between the Coulomb energy of two excess electrons occupying closely spaced (in the vertices of the square situated on one its side) positions and the energy of the electrons located in the far apart (in the vertices disposed along the diagonal) sites. In such case called "strong U approximation" the DE proves to be partially suppressed by the Coulomb repulsion producing self-trapping effect, and so the residual DE can be described by an effective second-order DE parameter $\tau = t^2/U$. Such coupling has been shown to result in the stabilization of the state in which the spins of both dimeric half-cells are maximal. This is in agreement with the fact that the DE in each dimeric subunit always acts as a ferromagnetic interaction. If the HDVV exchange between the d^n and d^{n+1} ions is antiferromagnetic (the most typical situation) it competes with the ferromagnetic second-order DE and so the ground spin-state of the cell appears to be dependent on the ratio $\tau/|J|$, where J is the parameter of the HDVV exchange. Finally, the quadrupole electrostatic field induced by the polarized driver-cell produces antiferromagnetic effect leading under some conditions to the spin-switching accompanied by the diminishing of the dimeric spin values.[31] This shows that the exploration of the spin degrees of freedom provides such useful function as spin-switching in addition to the function of QCA.

In this work we extend and complete the previous exploratory study[37] by presenting the detailed parametric theory of the multielectron cells exhibiting DE and HDVV exchange. We issue from the same electronic model as in the previous study but now along with the electronic interactions we also take into account vibronic coupling and analyze its effects on the key characteristics of QCA and also on the possibility of obtaining an additional spin switching function within the same device.

View Article Online
DOI: 10.1039/D1CP00444A

2. The model and main interactions

Let us preliminary summarize the main interactions included in the model with the qualitative emphasis on their main physical roles, while the precise quantitative consideration will be given in the next Sections. We consider a square cell consisting of the two MV dimeric subunits each two containing magnetic ions an d extra electron (Figure 1). The model of a QCA cell includes the following basic interactions:

1) electron transfer processes over the magnetic cores which are confined to the dimeric subunits 1-2 and 3-4 (Fig.1) and results in the so-called double exchange interactions. The last is known to lead to the ferromagnetic spin alignment[51] in each dimeric cluster;

2) Heisenberg-Dirac-Van Vleck (HDVV) exchange coupling which is assumed to operate within the dimeric clusters. We assume that it is antiferromagnetic as in majority of exchange clusters studied in molecular magnetism. It is to be underlined that by definition the HDVV exchange act within definite localized spin configurations;

3) interelectronic Coulomb repulsion is a relevant interaction because in the systems with alternating number of electrons per site such as MV clusters, different localized configurations have different Coulomb energies. As distinguished from the traditional localized exchange systems, the interelectronic Coulomb repulsion cannot be treated as an additive constant and ruled out. The importance of the Coulomb repulsion is illustrated in Fig. 1 from which one can see that the diagonal charge configurations are energetically more beneficial than the neighboring ones, and therefore the physical role of the Coulomb repulsion is to stabilize these antipodal configurations. For this reason the electron transfer (or alternatively, DE) and the Coulomb repulsion are competitive;

4) vibronic coupling with the "breathing" vibrations localized at the redox sites is commonly invoked when discussing the properties of MV compounds. This interaction has distinct trapping effect and therefore restricts the mobility of the extra electrons competing thus with the DE that is just interrelated with the electron transfer;

5) bearing in mind discussion of the functional properties of the cell (that will be referred to as "working" cell) one has to take into account the action of the neighboring cell ("driver") that is aimed to control the binary information encoded in the "working cell. We thus arrive to the necessity to include in the theory the cell-cell interactions. Traditionally, it is assumed that the driver cell is "prepared" in a certain polarization state and the control over the working cell is realized through an effective external field. Under this assumption a rather complicated problem of the cell-cell interaction can be reduced to a more simple and tractable problem of the "working"

cell subjected to an external field whose symmetry and strength depends on the mutualdisposition of the cells. So, the interaction of the cell with the field of the driver is included in the model.

3. Double exchange and Heisenberg-Dirac-Van Vleck exchange in bi-dimeric square cell

As a system in which the spin states of the magnetic ions are involved into the game, we consider a bi-dimeric square cell composed of two $d^n - d^{n+1}$ dimers with $1 \le n \le 8$ in which both d^n and d^{n+1} ions are assumed to be the high-spin ones. MV clusters of such kind are known to exhibit the DE, a special mechanism of spin coupling, which results in the ferromagnetic spin alignment caused by the spin polarization of the spin systems caused by the delocalization of the excess electron. [51]

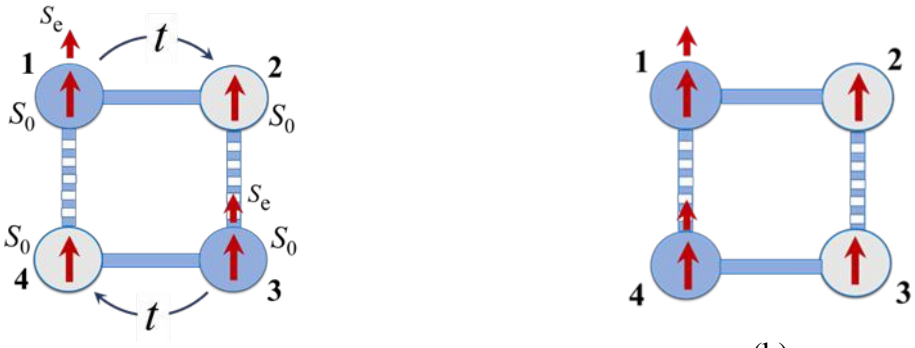

(a) (b)

Fig. 1. Bi-dimeric square cell (dimeric subunits 1-2 and 3-4) with one instant electronic distribution (d^n-ion for $1 \le n \le 4$ or d^{n+1}-ion for $n > 4$ is the spin core shown as gray circle, d^{n+1}-ion for $1 \le n \le 4$ or d^n-ion for $n > 4$ -blue circle): (a) distant charge localization minimizing Coulomb repulsion; (b) neighboring charge configuration having Coulomb energy U. S_0 is the spin of d^n and d^{n+1}-ions for the cases of $1 \le n \le 4$ and $n > 4$, respectively, arrow indicates the transfer of the excess electron (excess hole) provided that $1 \le n \le 4$ $(n > 4)$.

For $n \le 4$ we denote the spin of d^n-ion (spin cores) as S_0, then the spin of d^{n+1} ion is equal to $S_0 + 1/2$. We also denote the total spin values for the 1-2 and 3-4 dimers as S_{12} and S_{34}. In the case of $n \ge 5$ it is reasonable to deal with extra hole instead of extra electron. In this case d^{n+1}-ion (ion without extra hole) is regarded as spin core with the spin S_0 and the spin of d^n-ion possesses is equal to $S_0 + 1/2$. This is illustrated in Fig. 2 from which one can see that upon proper definition

View Article Online
DOI: 10.1039/D1CP00444A

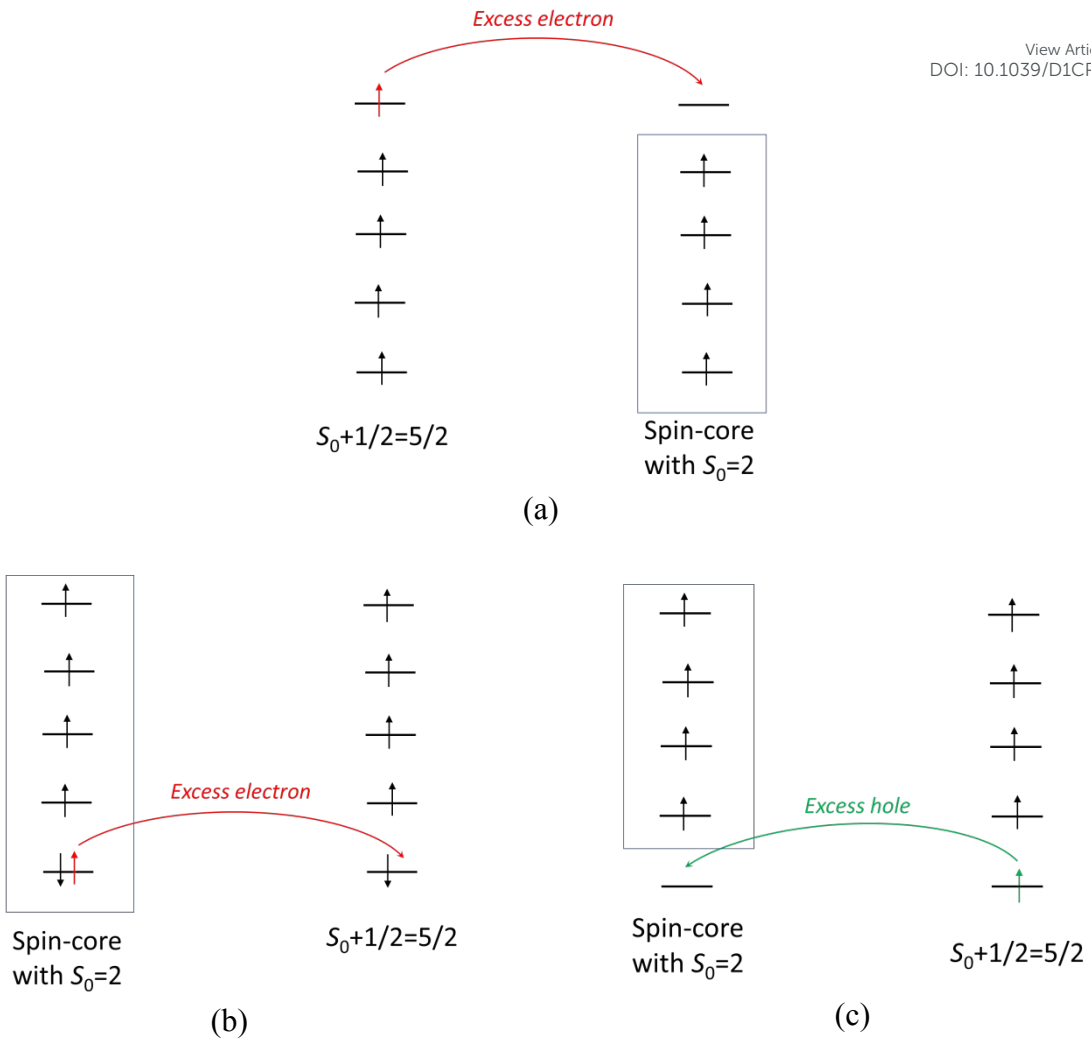

Fig. 2. Scheme of the electron transfer giving rise to the DE: (a) Electron transfer in the d^5-d^4-dimer exemplifying the case of less than half-filled d-shells; (b) Electron transfer in the d^6-d^5-dimer exemplifying the case of more than half-filled d-shells; (c) Hole transfer in the hole-type d^5-d^4-dimer that is equivalent to the electron transfer in the electron-type d^6-d^5-dimer. In all cases the core orbitals and the electrons or holes forming the spin-cores are shown in the box. It is assumed that the local crystal fields fully remove the degeneracies of the orbitals and both constituent ions are the high-spin ones.

of the spin core in all cases the spin of the excess particle (electron or hole) tends to be align in parallel with the spins S_0 of both spin cores which gives rise to the ferromagnetic spin alignment in the MV dimer. This fully agrees with the scheme shown in Fig. 1. It is worth noting that we restrict our consideration by the case of non-degenerate orbitals (see, for example, ref. [57] which deals with more general case when the orbital (special) degeneracy is involved).

In this Section we will focus on the first three interactions mentioned in Section 2, namely the DE, the intracell Coulomb interaction and the HDVV exchange. It is assumed that the electron

delocalization occurs only inside the dimeric fragments so that six charge configurations of the system is reduced to only four. The DE arises from the transfer of the excess electron in each dimer because in course of such transfer the excess electron polarizes the spin cores. Our consideration of the DE will be based on the assumption made in original DE model proposed by Zener [50] and further developed by Girerd and Papaefthymiou [53] according to which the energies of the non-Hund states are very high, i. e. the inequality $K >> |t|$ is fulfilled, in which K is the on-site exchange integral and t is the one-electron transfer parameter.

In this approximation the electronic Hamiltonian of the $d^n - d^{n+1}$ dimer in the position $i\,j$ (12 or 34) can be written as follows: [53]

$$\hat{H}_{ij} = \hat{H}_{DE}^{(i,j)} + \hat{H}_{EX}^{(i,j)} = B\hat{T}_{ij} - 2J\left(\hat{S}_i\hat{S}_j\hat{O}_i + \hat{S}_i\hat{S}_j\hat{O}_j\right), \quad (1)$$

where the operators $\hat{T}_{ij}$ and $\hat{O}_i$ are defined as follows:

$$\begin{aligned}
&\hat{T}_{ij}\left|(i)S_i^* = S_0 + 1/2, S_j = S_0, S_{ij}M_{ij}\right\rangle = \left|(j)S_i = S_0, S_j^* = S_0 + 1/2, S_{ij}M_{ij}\right\rangle,\\
&\hat{T}_{ij}\left|(j)S_i = S_0, S_j^* = S_0 + 1/2, S_{ij}M_{ij}\right\rangle = \left|(i)S_i^* = S_0 + 1/2, S_j = S_0, S_{ij}M_{ij}\right\rangle,\\
&\hat{O}_i\left|(i)S_i^* = S_0 + 1/2, S_j = S_0, S_{ij}M_{ij}\right\rangle = \left|(i)S_i^* = S_0 + 1/2, S_j = S_0, S_{ij}M_{ij}\right\rangle,\\
&\hat{O}_i\left|(j)S_i = S_0, S_j^* = S_0 + 1/2, S_{ij}M_{ij}\right\rangle = 0.
\end{aligned} \quad (2)$$

In Eq. (2) $\left|(i)S_i^* = S_0 + 1/2, S_j = S_0, S_{ij}M_{ij}\right\rangle$ and $\left|(j)S_i = S_0, S_j^* = S_0 + 1/2, S_{ij}M_{ij}\right\rangle$ are the wave-functions of the *i-j* MV dimer describing the states in which the excess electron is localized in the site *i* and *j* as indicated by symbols (i) and (j), S_i and S_j are the spins of the sites *i* and *j* provided that these sites are the d^n-ions ($S_i = S_j = S_0$), S_i^* and S_j^* are the spins of the d^{n+1} ions in the sites I and j ($S_i^* = S_j^* = S_0 + 1/2$), finally S_{ij} and M_{ij} are the total spin of the dimer and its projection.

The Hamiltonian, Eq. (1), includes two terms. The term $\hat{H}_{DE}^{(i,j)}$ is the Hamiltonian of the DE and the term $\hat{H}_{EX}^{(i,j)}$ describes the HDVV exchange interaction, where J is the parameter of the HDVV exchange interaction between the ions d^n and d^{n+1}, and B is the following DE parameter defined as:

$$B = t/(2S_0 + 1). \quad (3)$$

The DE operator $\hat{H}_{DE}^{(i,j)}$ links the wave-functions of the dimer belonging to the localization of the excess electrons in two different sites *i* and *j*. The corresponding matrix element proves to be dependent on the spin S_0 of the spin-core and on the total spin of the dimer S_{ij} due to the fact that the excess electron tends to polarize the spin cores in course of the transfer process. It follows from

View Article Online
DOI: 10.1039/D1CP00444A

Eqs. (1)-(3) that the matrix element of the DE is diagonal with respect to the quantum numbers S_{ij} and M_{ij}, and are given by the following expression:

$$\left\langle (j)S_i = S_0,\ S_j^* = S_0 + 1/2, S_{ij}M_{ij} \left| \hat{H}_{DE}^{(i,j)} \right| (i)S_i^* = S_0 + 1/2,\ S_j = S_0, S_{ij}M_{ij} \right\rangle = t\frac{S_{ij} + 1/2}{2S_0 + 1}. \quad (4)$$

The linear spin-dependence of the matrix element of the DE in Eq. (4) (and hence the linear spin-dependence of the corresponding energies) was first deduced by Anderson and Hasegawa [51] and represents one of the most important result of the theory of the DE,[51] which distinguishes the DE from the HDVV exchange giving rise to the quadratic spin-dependence of the energies of the dimer. It follows from Eq. (4) that the DE in a MV dimer always stabilizes the state with maximal spin, i. e. the DE acts as ferromagnetic interaction.

As in most cases we assume here that only one orbital in each site is accessible for the excess electron or hole (see Fig. 2). This assumption means that the ground terms of the constituent metal ions are orbitally non-degenerate. Going beyond this assumption leads to a significant complication of the energy spectrum of MV dimer, particularly, the DE has been shown to act as magnetically anisotropic interaction provided that the ground term of either d^{n+1} or d^n ion (or of both these ions) is an orbital triplet. [58, 59] Presently, we could not find a proper motivation (such as need to interpret experimental data) to extend the basic theory so far developed. On the other side, one can expect that the involvement of the orbitally degenerate ions can lead to the qualitatively new conclusions, such as new features interrelated with the magnetic anisotropy. For this reason, the case of orbital degeneracy in molecular QCA requires special consideration that is out of the scope of the present study.

The full DE operator of the bi-dimeric cell is defined as a sum of the DE operators of the constituent dimers, that is

$$\hat{H}_{DE} = \hat{H}_{DE}^{(1,2)} + \hat{H}_{DE}^{(3,4)}, \quad (5)$$

with each term of this sum being acting on only one excess electron. Let us present the DE Hamiltonian, Eq. (5), in the matrix form using as a basis the following set of the wave-functions of the bi-dimeric cell:

$$\left|(1,3)S_{12}M_{12}, S_{34}M_{34}\right\rangle \ \left|(2,4)S_{12}M_{12}, S_{34}M_{34}\right\rangle,\ \left|(1,4)S_{12}M_{12}, S_{34}M_{34}\right\rangle \text{ and } \left|(2,3)S_{12}M_{12}, S_{34}M_{34}\right\rangle$$

Here the short notations of the wave functions are used in which the spin-coupling schemes are not explicitly shown. Each of these wave-functions belongs to a definite set of spin quantum numbers $S_{12}, M_{12}, S_{34}, M_{34}$ and a definite occupation of the two electrons in the cell shown as a pairwise symbol (*i*, *j*) in which the first index *i* indicates the site of localization of the excess electron within the dimer 1-2, and the second index *j* specifies localization of the excess electron

belonging the dimer 3-4. Then, by using Eq. (4) and the properties of the additive operators one arrives at the following expressions for the matrix elements of the DE Hamiltonian, Eq. (5):

$$\begin{aligned}\left\langle (i,3)\,S_{12}M_{12},S_{34}M_{34}\left|\hat{H}_{DE}\right|(i,4)\,S_{12}M_{12},S_{34}M_{34}\right\rangle &= t\frac{(S_{34}+1/2)}{2S_0+1},\\ \left\langle (1,i)\,S_{12}M_{12},S_{34}M_{34}\left|\hat{H}_{DE}\right|(2,i)\,S_{12}M_{12},S_{34}M_{34}\right\rangle &= t\frac{(S_{12}+1/2)}{2S_0+1}.\end{aligned} \qquad (6)$$

In addition to the DE that forms the off-diagonal part of the full Hamiltonian matrix we will consider the two other interactions contributing to the diagonal part of the full Hamiltonian matrix, namely, the HDVV exchange which is described by the Hamiltonian $\hat{H}_{EX}=\hat{H}_{EX}^{(1,2)}+\hat{H}_{EX}^{(3,4)}$ the Coulomb repulsion between the excess electrons belonging to different MV dimers forming the cell. It is assumed that the HDVV exchange between the dimers is not operative as well as the DE. The matrix of the full Hamiltonian, which includes the DE term $\hat{H}_{DE}$, the intracell Coulomb repulsion term $\hat{H}_{CI}$ and the term $\hat{H}_{EX}$ describing the HDVV exchange has block-diagonal structure with each 4×4 block (according to the four types of the pair localizations) being correspond to the definite pair of quantum numbers S_{12}, S_{34}. Using Eq. (6) one obtains the following expression for each such block of the matrix:

$$\hat{H}(S_{12},S_{34})=\begin{pmatrix} E_{EX}(S_{12},S_{34}) & 0 & t\frac{(S_{34}+1/2)}{2S_0+1} & t\frac{(S_{12}+1/2)}{2S_0+1}\\ 0 & E_{EX}(S_{12},S_{34}) & t\frac{(S_{12}+1/2)}{2S_0+1} & t\frac{(S_{34}+1/2)}{2S_0+1}\\ t\frac{(S_{34}+1/2)}{2S_0+1} & t\frac{(S_{12}+1/2)}{2S_0+1} & U+E_{EX}(S_{12},S_{34}) & 0\\ t\frac{(S_{12}+1/2)}{2S_0+1} & t\frac{(S_{34}+1/2)}{2S_0+1} & 0 & U+E_{EX}(S_{12},S_{34}) \end{pmatrix}, \qquad (7)$$

where the intracell Coulomb energy U is defined as the difference in the repulsion energies of the two excess electrons occupying neighboring (1-4 and 2-3) and remote (1-3, 2-4) sites in a square cell as shown in Fig. 1. In Eq (7) the term

$$E_{EX}(S_{12},S_{34})=-J\left[S_{12}(S_{12}+1)+S_{34}(S_{34}+1)-2S_0(2S_0+3)-3/2\right] \qquad (8)$$

is the HDVV exchange energy representing the eigenvalue of the HDVV exchange Hamiltonian $\hat{H}_{EX}$ of the bi-dimeric cell. The matrix in Eq. (7) is a block of the full matrix related to a definite set of spin projections. In the subsequent analysis we will assume that $J<0$ (antiferromagnetic HDVV exchange) that is the most typical situation in clusters of transition metal ions. In this case the ferromagnetic DE and the antiferromagnetic HDVV exchange act as competitive interactions.

View Article Online
DOI: 10.1039/D1CP00444A

Note that $E_{EX}\left(S_{12},S_{34}\right)$ is independent of the distributions of the two excess electrons within the cell (i. e. the matrix of the HDVV exchange for each set of spin quantum numbers is proportional to the unit matrix in full accord with Eq. (7)) because for each allowed distribution the ion with the spin $S_0+1/2$ interacts with the ion having the spin S_0 within each constituent dimer. The quantum numbers of the spin-projections are omitted in the notation of the block $\hat{H}\left(S_{12},S_{34}\right)$ since the matrix elements of all above discussed interactions are independent of these quantum numbers.

Let us first consider a simplest case of cell composed of d^1-d^2 dimers, i. e. the case of one-electron spin cores ($S_0 = 1/2$). We will also assume at this stage that the HDVV exchange is negligibly weak. By setting $J = 0$ in Eq. (8) we find the energy levels of the cell shown in Fig. 3. Left part of Fig. 3 ($U = 0$) shows the set of the levels $E_{DE}(S_{12},S_{34}) = \pm t(S_{12}+S_{34}+1)/(2S_0+1)$ of the two non-interacting d^1-d^2 dimers. With the increase of the Coulomb repulsion the energy levels are grouped into the two sets separated by the energy gap that is of the order of U provided that U exceeds considerably the DE. In this limit one can observe an important effect of the reduction of the DE by the Coulomb repulsion. In fact, as one can see from Fig. 3 within each set of the well separated groups of the levels the DE is effectively reduced. The effect of reduction is caused by localization of the system in the favorable antipodal configurations minimizing the Coulomb repulsion that prevents polarization of the spin cores in the dimers by the excess electrons. Actually, the case of strong U is most relevant for functioning of the cell because just under this condition the information can be encoded in the two distinct antipodal charge distributions. For this reason, further on we will focus on this case and consider low lying Coulomb manifold well separated from the excited one. This low-lying group of levels is shown in the right side of Fig. 3 along with the symbolical picture of the corresponding populations of the sites.

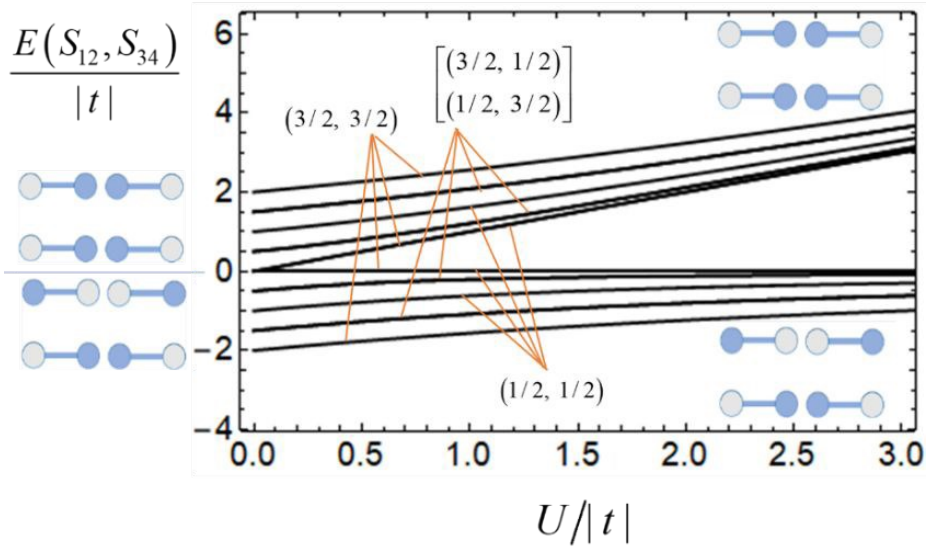

Fig. 3. Combined effect of the DE and intracell Coulomb repulsion on the energy levels of a square planar cell composed of two MV d^1-d^2 (or d^8-d^9) dimers. The energies are labeled by the set of quantum numbers (S_{12},S_{34}). Site of localizations-blue balls.

4. Full electronic Hamiltonian of a bi-dimeric square cell in a strong - *U* approximation

Up to now no restrictions on the relative strength of the three considered electronic interactions, described by the parameters U, t and J have been assumed. The subsequent consideration will be given for the most topical case of strong Coulomb repulsion when $U >> |t|, |J|$ (termed "strong U approximation" [60, 61]). In this case one can use the perturbation theory, by considering the Coulomb interaction Hamiltonian $\hat{H}_0 = \hat{H}_{CI}$ as an unperturbed Hamiltonian, and the Hamiltonian $\hat{H}_{PT} = \hat{H}_{HDVV} + \hat{H}_T$ as perturbation. This means that one can pass from the initial 4×4-matrix with the S_{12}, S_{34} - blocks to the effective matrix with twice smaller dimension which is also of block-diagonal structure, with each 2×2 S_{12}, S_{34} - block defined in the basis $\left|(1,3)S_{12},S_{34}\right\rangle, \left|(2,4)S_{12},S_{34}\right\rangle$.

By using the perturbation procedure up to the second order one obtains the following expression of the off-diagonal matrix element the effective Hamiltonian:

$$\begin{aligned}
&\left\langle(1,3)S_{12},S_{34}\left|\hat{H}_{eff}\right|(2,4)S_{12},S_{34}\right\rangle \\
&= -\frac{1}{U}\left\langle(1,3)S_{12},S_{34}\left|\hat{H}_{DE}\right|(2,3)S_{12},S_{34}\right\rangle\left\langle(2,3)S_{12},S_{34}\left|\hat{H}_{DE}\right|(2,4)S_{12},S_{34}\right\rangle \\
&\quad -\frac{1}{U}\left\langle(1,3)S_{12},S_{34}\left|\hat{H}_{DE}\right|(1,4)S_{12},S_{34}\right\rangle\left\langle(1,4)S_{12},S_{34}\left|\hat{H}_{DE}\right|(2,4)S_{12},S_{34}\right\rangle \\
&\quad = -\frac{2\tau\left(S_{12}+1/2\right)\left(S_{34}+1/2\right)}{\left(2S_0+1\right)^2},
\end{aligned} \tag{9}$$

where the parameter

$$\tau \equiv t^2/U \tag{10}$$

can be regarded as a second-order DE parameter. The diagonal matrix element $\left\langle(1,3)S_{12},S_{34}\left|\hat{H}_{eff}\right|(1,3)S_{12},S_{34}\right\rangle$ of the effective Hamiltonian is obtained as follows:

View Article Online
DOI: 10.1039/D1CP00444A

$$\begin{aligned}&\langle (1,3)S_{12},S_{34}|\hat{H}_{eff}|(1,3)S_{12},S_{34}\rangle = \langle (1,3)S_{12},S_{34}|\hat{H}_{EX}|(1,3)S_{12},S_{34}\rangle \\ &-\frac{1}{U}\langle (1,3)S_{12},S_{34}|\hat{H}_{DE}|(2,3)S_{12},S_{34}\rangle\langle (2,3)S_{12},S_{34}|\hat{H}_{DE}|(1,3)S_{12},S_{34}\rangle \\ &-\frac{1}{U}\langle (1,3)S_{12},S_{34}|\hat{H}_{DE}|(1,4)S_{12},S_{34}\rangle\langle (1,4)S_{12},S_{34}|\hat{H}_{DE}|(1,3)S_{12},S_{34}\rangle \\ &= E_{EX}(S_{12},S_{34}) - \frac{\tau}{(2S_0+1)^2}\left[(S_{12}+1/2)^2+(S_{34}+1/2)^2\right],\end{aligned} \tag{11}$$

and the same result is found for the matrix element $\langle (2,4)S_{12},S_{34}|\hat{H}_{eff}|(2,4)S_{12},S_{34}\rangle$.

Keeping in mind the QCA applications, we will assume that a given "working cell" (cell **1**) is subjected to a quadrupole electrostatic field created by the neighboring polarized "driver-cell" (cell **2**). The assumed mutual disposition of these two cells is shown in Fig. 4. Within the

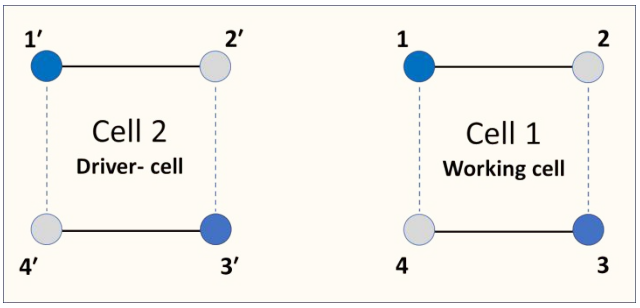

Fig. 4. Mutual in-plane disposition of the two bi-dimeric square cells: the working cell **1** and the polarized driver cell **2.** The latter cell creates the quadrupole electrostatic field acting on the working cell**.** The same coloring as in Fig. 1 is used for the spin cores and for sites with accommodated excess particle (electron or hole). The distribution of the four charges within the two interacting cells shown in the figure corresponds to the minimum of the interelectronic Coulomb energy of the two-cell moiety.

strong-U approximation, and making also reasonable assumption that the intracell Coulomb interaction considerably exceeds the intercell Coulomb interaction, the Stark interaction of the working cell with quadrupole field induced by the driver-cell has been shown to be described by the following 2×2 matrix defined in the $|(1,3)S_{12},S_{34}\rangle$ $|(2,4)S_{12},S_{34}\rangle$ - basis:

$$\hat{H}_{Stark} = -u\,P_2\hat{\sigma}_z, \tag{12}$$

where $\hat{\sigma}_z = \begin{pmatrix}1 & 0\\ 0 & -1\end{pmatrix}$ is the Pauli matrix, u is the parameter of the intercell Coulomb interaction defined as in [29, 30], and P_2 is the driver cell polarization, which is defined as

$$P_2 = \frac{\rho'_{13}-\rho'_{24}}{\rho'_{13}+\rho'_{24}}, \tag{13}$$

View Article Online
DOI: 10.1039/D1CP00444A

provided that the strong U approximation is fulfilled. In Eq. (13) ρ'_{13} and ρ'_{24} are the probabilities (electronic densities) of the two diagonal localizations of the electronic pair in the driver cell. Note that the strong U approximation implies that $\rho'_{13}+\rho'_{24}=1$. It is assumed that P_2 can change in a controllable manner from $P_2=-1$ (fully polarized state with $\rho'_{13}=0,\ \rho'_{24}=1$) to $P_2=+1$ (fully polarized state with $\rho'_{13}=1,\ \rho'_{24}=0$) passing through the unpolarized fully delocalized state with $P_2=0$ in which the electronic pair is equally distributed over two diagonal positions $\left(\rho'_{13}=\rho'_{24}=1/2\right)$.

Now we can write down the matrix of the full electronic Hamiltonian $\hat{H}_{EL}$ of the cell by combining the matrix of the effective Hamiltonian whose matrix elements are given by Eqs. (9) and (11) with the matrix of the Stark interaction, Eq. (12). Note that

$$-\frac{\tau}{\left(2S_0+1\right)^2}\left[\left(S_{12}+1/2\right)^2+\left(S_{34}+1/2\right)^2\right]=-\frac{\tau}{2\left(2S_0+1\right)^2}-\frac{\tau}{\left(2S_0+1\right)^2}\left[S_{12}\left(S_{12}+1\right)+S_{34}\left(S_{34}+1\right)\right], \quad (14)$$

and hence the diagonal contribution of the second-order DE gives rise to the same spin-dependence as the HDVV exchange coupling. Combining these two contributions and adding the Stark term we obtain the following 2×2 S_{12}, S_{34}-block of the matrix of the full electronic Hamiltonian:

$$\begin{aligned}\hat{H}_{EL}^{S_{12},S_{34}}=&-\left[\frac{\tau}{\left(2S_0+1\right)^2}-|J|\right]\left[S_{12}\left(S_{12}+1\right)+S_{34}\left(S_{34}+1\right)\right]\hat{\sigma}_0\\&-\frac{2\tau\left(S_{12}+1/2\right)\left(S_{34}+1/2\right)}{\left(2S_0+1\right)^2}\hat{\sigma}_x-u\,P_2\hat{\sigma}_z,\end{aligned} \quad (15)$$

where $\hat{\sigma}_0=\begin{pmatrix}1&0\\0&1\end{pmatrix}$, and $\hat{\sigma}_x=\begin{pmatrix}0&1\\1&0\end{pmatrix}$ are the Pauli matrices. While writing down Eq. (15) the common spin-independent energy shift $-\tau/2(2S_0+1)^2+2J\left[3/4+S_0(3+2S_0)\right]$ has been omitted.

The quadrupole electrostatic field of the polarized driver-cell induces polarization P_1 of the working cell. Within the strong U - approximation the polarization P_1 of the working cell can also be defined by Eq. (13) in which electronic densities ρ'_{13} and ρ'_{24} related to the driver-cell are substituted by the densities ρ_{13} and ρ_{24} of the electronic pair inside the working cell. The latter densities can be found by evaluating the wave-functions of the working cell (eigen-functions of the energy matrix, Eq. (15)). Since the densities ρ_{13} and ρ_{24} are functions of driver-cell

View Article Online
DOI: 10.1039/D1CP00444A

polarization P_2, the polarization P_1 is also dependent on P_2. The $P_1(P_2)$ - dependence, which is known as "cell-cell response function" represents one of the most important functional characteristics of QCA.[7] In what follows we will analyze both the evaluated dependences of the energies of the working cell on the deriver-cell polarization P_2 and the cell-cell response functions.

5. Conditions for stabilization of different electronic spin-states of the cell

In this section, we will look at the spin states of an isolated cell and then we will see how the driver field changes these states. The eigenvalues of the Hamiltonian, Eq. (15), are the following:

$$E_{\pm}^{S_{12},S_{34}}(P_2) = -\left[\frac{\tau}{(2S_0+1)^2} - |J|\right]\left[S_{12}(S_{12}+1) + S_{34}(S_{34}+1)\right] \pm \sqrt{u^2 P_2^2 + \frac{4\tau^2 (S_{12}+1/2)^2 (S_{34}+1/2)^2}{(2S_0+1)^4}}. \quad (16)$$

Let us first consider the case of isolated (free) cell when $P_2 = 0$ and hence the quadrupole field is also zero. One can see from Eq. (16) that the second-order DE gives ferromagnetic contribution to the overall exchange parameter and hence HDVV exchange and DE are in competition. Therefore, the spin quantum numbers S_{12} and S_{34} in the ground spin-state are determined by the relative strength of the second-order DE and HDVV exchange.

It follows from Eq. (16) that the HDVV exchange and the diagonal contribution of the second-order DE give the same spin-dependence. This is not surprising because the kinetic exchange and the second-order DE both represent the second-order contributions with respect to the electron transfer. At the same time a significant physical difference between the kinetic exchange and the diagonal part of the second-order DE should be underlined. Indeed, the kinetic exchange arises due to the electron transfer between the two half-occupied metal orbitals, which mixes the ground electronic configuration of the dimer with the excited charge-transfer configuration in which the two electrons occupy the same orbital on the same metal site. Due to the Pauli principle such mixing gives rise to the antiferromagnetic exchange coupling that is described by the exchange parameter proportional to t^2/U_0, where U_0 is the on-site Coulomb energy. Such antiferromagnetic kinetic exchange is obtained from the Hubbard Hamiltonian provided that $U_0 >> t$. In contrast, the effective DE Hamiltonian is associated with the electron transfer from the half-filled orbital to the empty orbital, which leads to the Coulomb excitation by the the energy U representing, as distinguished from U_0, the inter-site Coulomb energy. Up to the

View Article Online
DOI: 10.1039/D1CP00444A

second-order of perturbation theory such effective DE is described by the parameter $\tau = t^2/U$. The mixing of the ground and excited Coulomb manifolds caused by such transfer is not affected by the Pauli principle, and so the effect of the second-order DE proves to be ferromagnetic. Note that the first-order DE in a MV dimer is in most cases much stronger than the HDVV exchange ($t >> |J|$) favoring thus the ferromagnetic ground state of the dimer. Unlike this, in a bi-dimeric cell when the DE acts as a second-order interaction it can be comparable with the HDVV exchange, and the ground spin-state of the cell is determined by the competition of these two interactions.

By analyzing Eq. (16) one can prove that the ground state of the free cell possesses minimal spin values $S_{12} = 1/2, S_{34} = 1/2$ provided that

$$\tau/|J| < (2S_0 + 1)^2/2, \qquad (17)$$

and maximal spin values $S_{12} = 2S_0 + 1/2, S_{34} = 2S_0 + 1/2$ otherwise.

The above found conditions are illustrated by the correlation diagram plotted in Fig. 5a for the simplest case of the isolated cell composed of two d^1-d^2 (or d^8-d^9) dimers. It is seen that for relatively strong HDVV exchange coupling ($\tau/|J| < 2$) the ground state possesses minimal spin values for the constituent dimeric half-cells $(S_{12} = S_{34} = 1/2)$, while for weak HDVV exchange

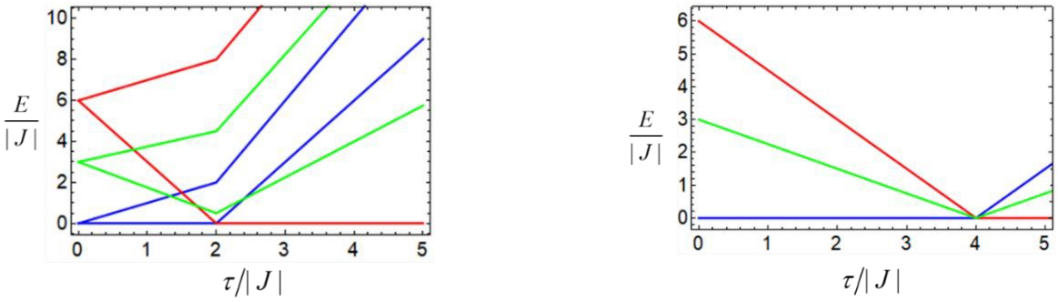

Fig. 5. Correlation diagrams for bi-dimeric square cell composed of d^1-d^2 (or d^8-d^9) dimers evaluated at $uP_2 = 0$ (a) and at $u|P_2| >> \tau$ (b). Coloring: $S_{12} = S_{34} = 1/2$ - blue lines, $S_{12} = S_{34} = 3/2$ -red lines, $S_{12} = 1/2(3/2), S_{34} = 3/2(1/2)$ - green lines. The energy of the ground state is regarded as a reference energy.

coupling ($\tau/|J| > 2$) the ground state has maximal dimeric spin values $(S_{12} = S_{34} = 3/2)$. Finally, at $\tau/|J| = 2$ these two states become degenerate. As to the states in which one dimer has the spin 1/2 while another dimer is that with the spin 3/2, such states prove to be always excited.

When the quadrupole Coulomb field of the driver-cell is nonzero it tends to polarize the electronic pair in the working cell thus suppressing the off-diagonal part of the ferromagnetic second-order DE. Mathematically this follows from the fact that the off-diagonal part of the

second-order DE and the inter-cell Coulomb interaction are described by non-commuting matrices (see Eq. (15)) and hence these two interactions are in competition. This means that the field of the driver cell weakens the ferromagnetic effect caused by the second-order DE. In other words, the field of the driver produces additional antiferromagnetic effect enhancing thus the antiferromagnetic effect induced by the HDVV exchange. In the limit of strong driver field defined by the inequality $\frac{\tau}{u|P_2|} << 1$, the resonance second-order DE term in Eq. (16) is fully suppressed and the expression for the energies acquires the following form:

$$E_{\pm}^{S_{12},S_{34}}(P_2) \approx -\left[\frac{\tau}{(2S_0+1)^2} - |J|\right]\left[S_{12}(S_{12}+1)+S_{34}(S_{34}+1)\right] \pm u|P_2|. \quad (18)$$

It follows from Eq. (18) that the ground state of the cell subjected by the action of extremely strong quadrupole field possesses the minimal spin values $S_{12}=1/2, S_{34}=1/2$ for

$$\tau/|J| < (2S_0+1)^2, \quad (19)$$

and the maximal spin values $S_{12}=2S_0+1/2, S_{34}=2S_0+1/2$ otherwise. Finally, for $\tau/|J| = (2S_0+1)^2$ the ground state proves to be highly degenerate and comprises all possible combinations of dimeric spins S_{12} and S_{34}. By considering together the conditions defined by Eqs. (17) and (19), we arrive at the conclusion that irrespectively of the strength of the quadrupole field the ground state of the bi-dimeric working cell possesses minimal S_{12} and S_{34} values for

$$\tau/|J| < (2S_0+1)^2/2, \quad (20)$$

and maximal such values for

$$\tau/|J| > (2S_0+1)^2 \quad . \quad (21)$$

In contrast, if the condition

$$(2S_0+1)^2/2 < \tau/|J| < (2S_0+1)^2 \quad (22)$$

is fulfilled, the ground state proves to be dependent on the strength of the field, namely this state possesses maximal spin values for weak field and minimal spin values for strong such field. Note that the usage of the last condition requires some precaution, because the maximal quadrupole field induced by the polarized driver-cell is limited by the distance between the neighboring cells. In fact, this distance should not be too short in order to effectively isolate these cells precluding thus from the electron transfer and the exchange coupling between the cells. Under these circumstances even such maximal field can happen to be not enough to cause the spin-switching.

Figure 5b shows the correlation diagram related to the case of cell composed of two d^1-d^2 (or d^8-d^9) dimers which is subjected by extremely strong quadrupole field. It is seen that for

$\tau/|J|<4$ the ground state of the cell in this limit has minimal spin values S_{12}, S_{34}, for $\tau/|J|>4$ this state possesses maximal spin values, finally, provided that $\tau/|J|=4$ the ground state is degenerate and comprises all pairs S_{12}, S_{34}. By comparing this correlation diagram with that for the free cell (Fig. 5a) we arrive at the conclusion that the ground state of the cell always (irrespectively of the strength of quadrupole field) has minimal dimeric spin values for $\tau/|J|<2$ and maximal dimeric spin values for $\tau/|J|>4$, while for $2<\tau/|J|<4$ this state can exhibit spin switching $S_{12}=S_{34}=1/2 \rightarrow S_{12}=S_{34}=3/2$ upon increasing of the field in agreement with the above found general conditions (20)-(22) in which one should set $S_0=1/2$.

6. Effect of the driver-cell field on the spin-states and polarization of the working cell

Now we are in position to test the influence of the quadrupole field of the driver cell on the energy levels and polarization of the working cell. As illustrative example, which retains key features of the phenomena and gives at the same time clear pictural representation we consider a simplest example of the bi-dimerc cell composed of d^1-d^2 (or d^8-d^9) subunits. Left column in Fig. 6 shows the low-lying electronic energy levels of the working cell as functions of polarization P_2 of the driver-cell evaluated at fixed values of the second-order DE $\tau = 40\ \mathrm{cm}^{-1}$, Coulomb energy $u = 250\ \mathrm{cm}^{-1}$, and with a variable parameter J of HDVV exchange.

The corresponding cell-cell response functions $P_1(P_2)$ calculated in the low-temperature limit (i. e. with account of only the ground spin-state) in the framework of the electronic model are shown by solid lines in the right column in Fig. 6. While discussing the results emanating from the electronic model one should consider the curves corresponding to the vibronic coupling parameter υ=0, while the vibronic effects will be considered in the next Sections.

The calculated dependences confirm the above statement concerning the antiferromagnetic effect of the quadrupole driver's field. Indeed, as one can see from Fig. 6, the increase of P_2 always leads to the stabilization of the low-lying state having $S_{12}=S_{34}=1/2$ with respect to the states

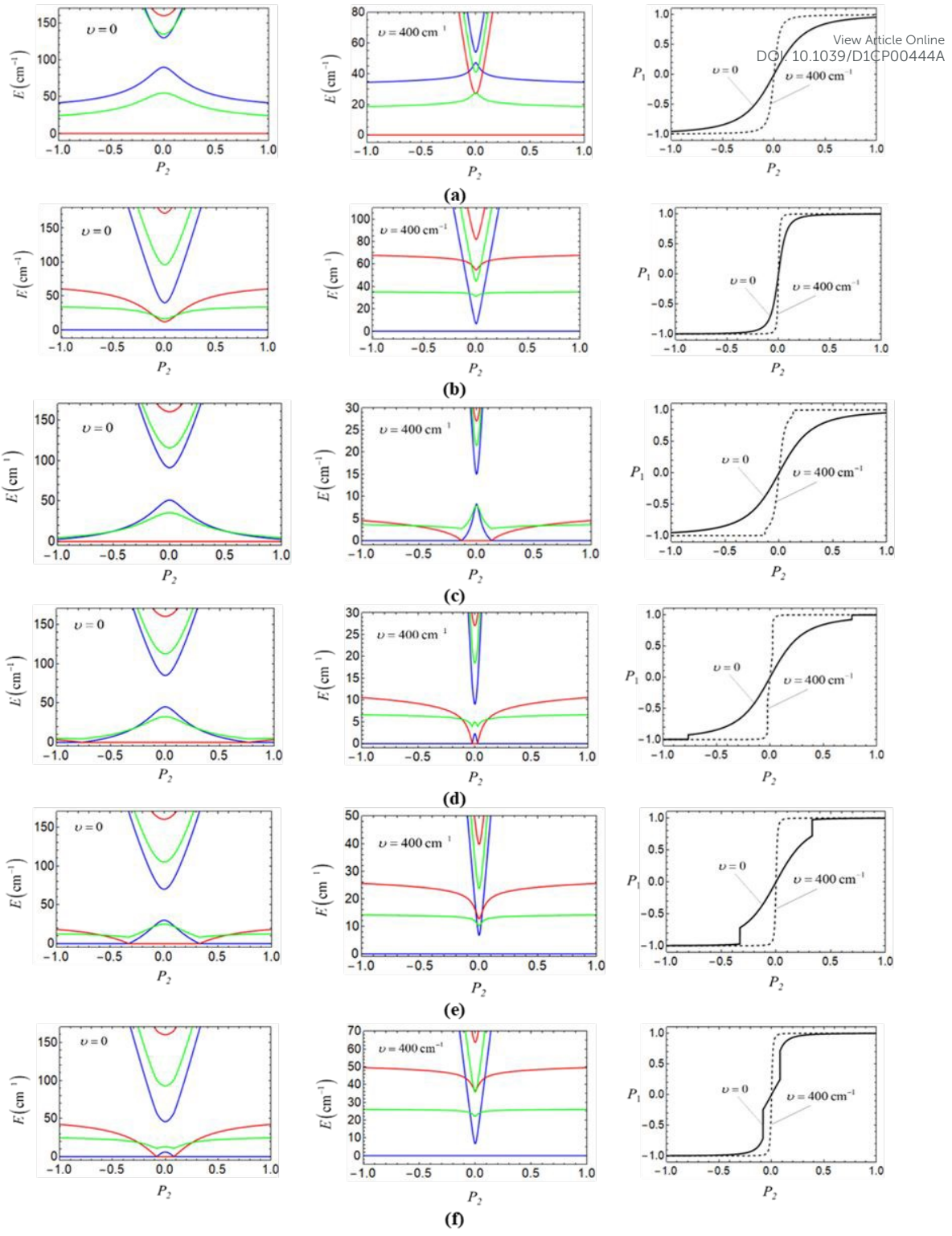

Fig. 6. Effect of the quadrupole field of the driver-cell with polarization P_2 on the energies E and polarization P_1 of the working cell evaluated with $u = 250\ \mathrm{cm}^{-1}$, $\tau = 40\ \mathrm{cm}^{-1}$, $\hbar\omega = 300\ \mathrm{cm}^{-1}$, two values of the vibronic coupling parameter υ (0 and 400 cm^{-1}) shown in the plots and $J = -5\ \mathrm{cm}^{-1}$ (a), $-22\ \mathrm{cm}^{-1}$ (b), $-11.5\ \mathrm{cm}^{-1}$ (c), $-12.5\ \mathrm{cm}^{-1}$ (d), $-15\ \mathrm{cm}^{-1}$ (e), $-19\ \mathrm{cm}^{-1}$ (f). The same coloring as in Fig. 5 is used. The energy of the ground state is chosen as the reference energy.

View Article Online
DOI: 10.1039/D1CP00444A

with $S_{12} = S_{34} = 3/2$ and with $S_{12} = 1/2(3/2)$, $S_{34} = 3/2(1/2)$. When the driver-cell is getting fully polarized (i. e. at $|P_2|=1$) the induced polarization $|P_1|$ of the working cell tends to 1 and the relative energies tend to those given by Eq. (18), which corresponds to the strong field limit.

We start the discussion of the effects of the driver field with the cases when such field is unable to cause the spin-switching in the working cell. As has been shown in the previous section these are the cases when $\tau/|J|>4$ and $\tau/|J|<2$. These two cases are illustrated in Figs. 6a and 6b.

When $\tau/|J|>4$ the ground state belongs to the spin states $S_{12} = S_{34} = 3/2$ even provided that the driver-cell is fully polarized (Fig. 6a, left column), although the energy gaps between this state and the excited states with $S_{12} = 1/2(3/2), S_{34} = 3/2(1/2)$ and $S_{12} = S_{34} = 1/2$ found at $|P_2|=1$ are considerably smaller than those occurring at $P_2 = 0$. It is seen (Fig. 6a, right column, solid line) that the $P_1(P_2)$-dependence in this case is rather gradual (with a gentle slope) and hence such case is not favorable for QCA functioning. Such gradual behavior of cell-cell response function is explained by the fact that the DE splitting is larger for larger dimeric spin values, and hence the Stark effect for such state proves to be weaker. In other words, the electron delocalization giving rise to the DE, precludes from efficient polarization of the excess electrons by the quadrupole field of the driver-cell, and so the cell in the $S_{12} = S_{34} = 3/2$-state proves to be less polarizable than the cell having smaller S_{12}, S_{34} values.

In contrast, for $\tau/|J|<2$ the ground state of the isolated cell always has $S_{12} = S_{34} = 1/2$ (Fig. 6b, left column), and the field of the polarized driver-cell only additionally stabilizes this state with respect to the excited ones with larger spin values. In this case the Stark effect is much stronger and hence it gives rise to strongly nonlinear $P_1(P_2)$ dependence with steep slope (Fig. 6b, right column, solid line). This means that such case is favorable for functioning of QCA-based devices.

Now let us proceed to the discussion of the case when the ground spin-state of the cell in the strong field limit is different from that for the free cell, which occurs provided that $2<\tau/|J|<4$. This situation is shown in Figs. 6 c-f. At relatively weak HDVV exchange the ground state at $|P_2|=1$ is still possesses $S_{12} = S_{34} = 3/2$ (Fig. 6c, left column) but the energy gaps between this level and the first and second excited levels with smaller dimeric spins are strongly diminished as compared with the corresponding zero-field gaps. This means that at given *u* value (which seems to be reasonable, as will be discussed below) even the maximally possible quadrupole field arising at $|P_2|=1$ is still not enough to cause the spin-switching. For this reason, the cell-cell response

function in this case proves to be exactly the same as for the above discussed case of $\tau/|J|>4$ (Fig. 6a, right column, solid line) provided that in both cases τ is fixed at $40\ \mathrm{cm}^{-1}$. This result has a clear physical sense, indeed, in the framework of the pure electronic model the cell-cell response can depend only on the parameter τ determining the strength of the Stark effect but not on $|J|$ except the cases when the change of $|J|$ leads to the change of the ground spin-state. At smaller ratios $\tau/|J|$ (Figs. 6d-6f) the quadrupole Coulomb field of enough strength causes the switching of the ground state from $S_{12}=S_{34}=3/2$ to $S_{12}=S_{34}=1/2$ (Figs. 6d-6f, left column). As a result, the evaluated electronic cell-cell response functions show non-monotonic behavior due to spin-switching between the two spin-states exhibiting different polarizabilities (Figs. 6d-6f, right column, solid line). Note that the smaller is the ratio $\tau/|J|$ the weaker is the polarization of the driver-cell required to cause such spin-switching (compare Figs. 6d, 6e and 6f) because the zero-field gap between the states with $S_{12}=S_{34}=3/2$ and $S_{12}=S_{34}=1/2$, that is to be overcome by the quadrupole field, is smaller for smaller $\tau/|J|$.

At this stage, it seems appropriate to briefly discuss to which extent the values of the parameters we use in our calculations and the conditions implied by strong-U approximation are compatible with the situation in real systems. Note, that the value $\tau = 40\ \mathrm{cm}^{-1}$ used in the plots in Fig. 6 falls within its range determined by using the t values found for some recently reported weakly coupled MV clusters. [48, 49] Thus for $[Fe_2]^V$ complex $t \approx 416\ \mathrm{cm}^{-1}$ and the Fe-Fe - distance is $\approx 8\ \mathrm{\AA}$.[49] For square cell composed of such dimers the estimated intracell Coulomb energy U proves to be $\approx 4235\ \mathrm{cm}^{-1}$ and so the inequality $t << U$ is fulfilled rather well, with the corresponding second-order DE parameter being equal to $\tau \approx 40.86\ \mathrm{cm}^{-1}$ that is close to the value $40\ \mathrm{cm}^{-1}$ we use in our calculations. Depending on the intermetallic distances and the bridging angles in the weakly coupled transition metal clusters the absolute value of the HDVV exchange parameter J typically vary from several wavenumbers [48, 49] to several tens of wavenumbers [45] and so the values of J used here and satisfying the condition $|J|<<U$ also fall within the reasonable range of values. Finally, the used value $u = 250\ \mathrm{cm}^{-1}$ can also be regarded as reasonable estimation of the intercell Coulomb energy for typical intra- and intercell distances. [37]

7. Vibronic coupling

The vibronic coupling is an inherent part of the problem of intramolecular electron transfer and mixed valency underlying the fundamental properties of MV compounds such as electron localization and intervalence optical bands. In view of the present consideration of molecular MV cell one should mention that the vibronic coupling was shown to produce a significant impact on

the functional properties of molecule-based QCA through the vibronic trapping of the charges carrying binary information. [36, 60-65] In this respect the question arises of how this interaction specifically affects the properties of the bi-dimeric cell exhibiting DE and HDVV exchange.

Hereunder the vibronic interaction will be considered in the framework of the Piepho, Krausz and Schatz (PKS) model traditionally used in chemistry and physics of MV compounds,[66] which involves the interaction of the mobile electrons with the full-symmetric local vibrations ("breathing" modes). The dimensionless vibrational coordinates for the breathing vibrations of the first coordination spheres of the sites 1, 2, 3 and 4 will be denoted as q_1, q_2, q_3, q_4. It is assumed within the PKS model that the frequencies of the breathing modes are site-independent and also equal for d^n and d^{n+1} ions. This common frequency will be denoted as ω. The matrix elements of the vibronic coupling are diagonal in the basis of each localized orbital 1, 2, 3 and 4 that allows to obtain the matrix of the full vibronic Hamiltonian in spin-coupled representation.

Now let us assume that the Coulomb energy U exceeds not only $|t|$ and $|J|$ but also it is much higher than the effective energy of the vibronic coupling which means that the "strong-U approximation" is applied to the vibronic model of the bi-dimeric cell. Within this assumption one can consider vibronic interaction as acting within the truncated basis of the low-lying states $\left|(1,3)S_{12},S_{34}\right\rangle$ and $\left|(2,4)S_{12},S_{34}\right\rangle$. Then the vibrationally-dependent contribution to the cell Hamiltonian can be defined as follows:

$$\hat{H}_{q_i}=\frac{\hbar\omega}{2}\sum_{i=1}^{4}\left(q_i^2-\frac{\partial^2}{\partial q_i^2}\right)\hat{\sigma}_0+\frac{\upsilon}{2}\left[(q_1+q_3)(\hat{\sigma}_0+\hat{\sigma}_z)+(q_2+q_4)(\hat{\sigma}_0-\hat{\sigma}_z)\right], \qquad (23)$$

where the first term represents the Hamiltonian for free harmonic oscillations and the second term describes a linear (with respect to the vibrational modes) vibronic coupling, which is characterized by the vibronic coupling parameter υ. The latter parameter is also assumed to be site-independent. The form of the vibronic term in Eq. (23) reflects the main assumption of the vibronic PKS model according to which different sites are vibronically independent. Then, the four independent local displacements q_1, q_2, q_3, q_4 can be transformed to the symmetry adapted coordinates $q_\alpha=\sum_{i\alpha}c_{i\alpha}q_i$ $(i=1,2,3,4)$ of a cell corresponding to the irreducible representations $\alpha=A_{1g},B_{1g},E_u$ of the point group D_{4h}. By passing to the symmetry adapted vibrations of the cell one finds:

$$q_{A_{1g}}=(q_1+q_3+q_2+q_4)/2,$$

$$q_{E_ux}=(q_1-q_3)/\sqrt{2},\quad q_{E_uy}=(q_2-q_4)/\sqrt{2}, \qquad (24)$$

$q_{B_{1g}} = (q_1 + q_3 - q_2 - q_4)/2$.

View Article Online
DOI: 10.1039/D1CP00444A

One can prove that within the used strong-U approximation the interactions of the excess electrons with all vibrations except the mode $q \equiv q_{B_{1g}}$ are described by the matrices which are proportional to the unit matrix and so they can be ruled out from the consideration. Keeping this in mind we arrive at the one-mode vibronic problem with the following vibrationally-dependent Hamiltonian:

$$\hat{H}_q = \frac{\mathsf{h}\omega}{2}\left(q^2 - \frac{\partial^2}{\partial q^2}\right)\hat{\sigma}_0 + \upsilon q\hat{\sigma}_z \,. \tag{25}$$

Now one can write down the following full Hamiltonian of the cell:

$$\hat{H}^{S_{12},S_{34}} = \hat{H}_{EL}^{S_{12},S_{34}} + \hat{H}_q \,, \tag{26}$$

which includes both electronic and vibronic interactions. The Hamiltonian, Eq. (26), can be significantly simplified in the adiabatic approximation when one neglects the vibrational kinetic energy, that is the term $-\frac{\mathsf{h}\omega}{2}\frac{\partial^2}{\partial q^2}$ in Eq. (25). Although the adiabatic approach is rather approximative [65] it can serve as an useful guide in the qualitative and partially semiquantitative description of the effect of the vibronic coupling on the functional properties of molecular QCA due to its simplicity and visibility. For these reasons we start from the semiclassical analysis and then will proceed to a more exact consideration based on the use of quantum-mechanical vibronic approach. In the adiabatic approximation one finds the following expressions for the eigenvalues of the Hamiltonian, Eq. (26):

$$\begin{aligned} U_{\pm}^{S_{12},S_{34}}(q) = &-\left[\frac{\tau}{(2S_0+1)^2} - |J|\right]\left[S_{12}(S_{12}+1) + S_{34}(S_{34}+1)\right] \\ &+ (\mathsf{h}\omega/2)\,q^2 \pm \sqrt{\frac{4\tau^2(S_{12}+1/2)^2(S_{34}+1/2)^2}{(2S_0+1)^4} + (\upsilon q - u P_2)^2} \,, \end{aligned} \tag{27}$$

which represent the adiabatic potentials of the working cell subjected to the field of the driver-cell.

8. Effect of the vibronic coupling on the spin states of the isolated cell: adiabatic approach

It was thoroughly discussed [54-56, 60-65] that the key effect of the vibronic coupling in MV clusters is a vibronic self-trapping effect arising from the fact that the extra electron produces deformation of the ligand surrounding near the redox site, so that the elastic energy gain exceeds the bonding energy arising from electron delocalization. From the mathematical point of view the

transfer term and the vibronic coupling are described by the non-commuting matrices and hence these two interactions are competitive and, in particular, the vibronic interaction tends to suppress the electron delocalization.

As a consequence, in the systems comprising spin cores the vibronic coupling tends to reduce the DE. In the present case when the DE acts as a second-order interaction described by the parameter τ the role of the vibronic coupling is to reduce the ferromagnetic effect caused by the off-diagonal terms of the second-order DE, while the diagonal DE terms remain unaffected by the vibronic coupling as well as the HDVV exchange due to the fact that corresponding energy matrices commute with each other. From this point of view the effect of the vibronic coupling is expected to be quite similar to the above considered effect of the quadrupole electrostatic field created by the polarized driver-cell. Keeping in mind these arguments one can expect that the vibronic coupling should produce an antiferromagnetic effect.

To prove this let us first analyze the spin-dependent energies $U_{-}^{S_{12},S_{34}}\left(q_{min}\right)$ of the minima of the lower sheet of the adiabatic potential of a free cell, i. e. provided that the quadrupole field acting on the working cell is zero (P_2 = 0). We will focus on the two limits, namely, negligibly weak vibronic coupling $\left(\upsilon=0\right)$ and strong vibronic coupling. We define the limit of strong vibronic coupling as a case when υ is much larger than the second order DE parameter τ but at the same time it is assumed that the vibronic coupling is still significantly smaller than both the Coulomb energy gap *U* and the transfer integral *t*. The latter condition means that as distinguished from the electron transfer mixing of the ground and excited Coulomb manifolds which are taken into account as a second order effect, the vibronic mixing of the ground and excited Coulomb manifolds can be fully neglected.

At $\upsilon=0$ the adiabatic potential curve $U_{-}^{S_{12},S_{34}}\left(q\right)$ represents a parabola in the point $q_{min}=0$, with the energy in this minimum being given by the same expression as the pure electronic zero-field energy $E_{-}^{S_{12},S_{34}}\left(P_2=0\right)$ evaluated with the aid of Eq. (14). If the vibronic coupling is strong enough to ensure the inequality $\upsilon^2/\mathrm{h}\omega > 2\tau\left(S_{12}+1/2\right)\left(S_{34}+1/2\right)/\left(2S_0+1\right)^2$, the curve $U_{-}^{S_{12},S_{34}}\left(q\right)$ possesses two equivalent minima at the points:

$$q_{min}^{\pm}\left(S_{12},S_{34}\right)=\pm\sqrt{\left(\frac{\upsilon}{\mathrm{h}\omega}\right)^2-\frac{4\tau^2\left(S_{12}+1/2\right)^2\left(S_{34}+1/2\right)^2}{\left(2S_0+1\right)^4\upsilon^2}}\,. \tag{28}$$

The minima of this double-well potential have the following energies:

View Article Online
DOI: 10.1039/D1CP00444A

$$U_{-}^{S_{12},S_{34}}\left[q=q_{min}^{\pm}\left(S_{12},S_{34}\right)\right]=-\frac{\upsilon^2}{2\mathsf{h}\omega}-\left[\frac{\tau}{\left(2S_0+1\right)^2}-|J|\right]\left[S_{12}\left(S_{12}+1\right)+S_{34}\left(S_{34}+1\right)\right]-\frac{2\tau^2\left(S_{12}+1/2\right)^2\left(S_{34}+1/2\right)^2\mathsf{h}\omega}{\left(2S_0+1\right)^4\upsilon^2}. \quad (29)$$

When $\tau << \upsilon$ the last term tends to zero and so in the strong vibronic coupling limit we obtain

$$U_{-}^{S_{12},S_{34}}\left[q=q_{min}^{\pm}\left(S_{12},S_{34}\right)\right]=-\frac{\upsilon^2}{2\mathsf{h}\omega}-\left[\frac{\tau}{\left(2S_0+1\right)^2}-|J|\right]\left[S_{12}\left(S_{12}+1\right)+S_{34}\left(S_{34}+1\right)\right]. \quad (30)$$

By comparing this energy with the energy $E_{-}^{S_{12},S_{34}}\left(P_2\right)$ of the ground state in Eq. (18) obtained for the strong quadrupole field limit, one can see that these two expressions differ only in the spin-independent terms (vibronic stabilization term $-\frac{\upsilon^2}{2\mathsf{h}\omega}$ in Eq. (30) and stabilization term $\pm u|P_2|$ in Eq. (18) arising from the field of the driver-cell), while the terms describing the spin-dependent splitting in Eqs. (18) and (30) prove to be identical. This finding reflects the deep analogy between the effects of the quadrupole field and the vibronic coupling consisting in the fact that both interactions tend to localize the excess electrons and hence to polarize the cell. Note, however, that as distinguished from the quadrupole field, which stabilizes the state with definite electric polarization, vibronic coupling leaves the ground state double degenerate (two energetically equivalent minima of the lowest adiabatic potential curves). This means that in the latter case one can speak about polarization of the cell only in the sense of broken symmetry, that is the cell is only polarized in one or another deep minimum, meanwhile the overall electric polarization remains of course zero provided that the quadrupole field is zero. Anyway, when the field is applied, it is able to much easier polarize the cell when the vibronic coupling is strong since the latter interaction takes over most of the work of polarizing the cell.

As far as the patterns of spin levels above obtained for the isolated cell in the limits of weak and strong vibronic coupling are shown to be exactly the same as those obtained in the limits of weak and strong quadrupole field in the framework of the electronic model, one can conclude that the conditions for stabilization of the different spin-states of the free cell in the presence of the vibronic coupling look quite similarly to the conditions expressed by Eqs. (20)-(22), obtained provided that the cell is subjected by the action of the field induced by the driver-cell and the vibronic coupling is negligibly weak. E. g., one finds for $\tau/|J|<\left(2S_0+1\right)^2/2$ and for $\tau/|J|>\left(2S_0+1\right)^2$ the ground state of the bi-dimeric cell is independent of the strength of the vibronic coupling and possesses minimal and maximal S_{12} and S_{34} values, respectively. In contrast,

View Article Online
DOI: 10.1039/D1CP00444A

for $(2S_0+1)^2/2 < \tau/|J| < (2S_0+1)^2$ the ground state proves to be dependent on the strength of the vibronic coupling, namely this state should possess maximal spin values for weak vibronic coupling and minimal spin values for strong such coupling.

10. Vibronic coupling: quantum-mechanical treatment of spin-vibronic states

The adiabatic approximation employed in the previous section works well for an isolated cell in the case of a strong vibronic coupling when the system (which belong to class I or partially at the borderline between the classes I and II in Robin &Day scheme) is strongly localized in the deep equivalent minima of the adiabatic potential. Under this condition the adiabatic approach is valid only for the states of the system near the bottom of the minima for which the quantum effect of tunneling is small that means that the tunnel splitting is much less than the vibrational frequency. This condition is much less favorable for the excited levels for which the tunneling is more efficient and finally for the states in the vicinity of the crossover of the adiabatic potentials the adiabatic approach fails even if the condition of strong vibronic coupling is fulfilled. Finally, in the case of a moderate vibronic coupling (class II) the adiabatic approach in inapplicable.

The conditions of the validity of the adiabatic approach so far qualitatively described for a free cell require important additional comment as applied to the cell subjected to the field of the driver. In fact, in the presence of the external field the minima of the lower sheet of the potential curves became non-equivalent so that at a certain field the adiabatic description of states in the shallow minimum fails due to fast tunneling. Just these non-adiabatic transitions are operative in the reorientation of the polarization of the cell and play a crucial role in the shape of the cell-cell response function. Moreover, one can conclude that the reorientation caused by quantum tunneling starts earlier (as function of the field) than the classical excitation over the barrier. It is to be underlined that this conclusion that is specific for the QCA application restricts the application of the adiabatic approach even provided that the vibronic coupling is strong. That is why in this section we explore the quantum-mechanical approach to the vibronic problem of the QCA cell and especially for the evaluation of the cell-cell response function.

We will analyze the energy levels of a free cell calculated as functions of the parameter υ. In these calculations instead of the usage of semiclassical adiabatic approximation we will issue from a more exact quantum-mechanical vibronic approach based on the numerical solution of the dynamic pseudo-Jahn-Teller (JT) vibronic problem arising upon involvement into consideration of the vibrational kinetic energy term $-\frac{\hbar\omega}{2}\frac{\partial^2}{\partial q^2}$. Within this approach the matrices of the full Hamiltonian $\hat{H}^{S_{12},S_{34}}$ are defined in the basis composed of the products $\left|(1,3)S_{12}M_{12},S_{34}M_{34}\right\rangle\left|n\right\rangle$

View Article Online
DOI: 10.1039/D1CP00444A

and $\left|(2,4)S_{12}M_{12},S_{34}M_{34}\right\rangle\left|n\right\rangle$ of the localized electronic wave-functions for two diagonal-types electronic distributions and the harmonic oscillator wave-functions ($n = 0, 1, \ldots$). By diagonalizing this matrix, one obtains the spin-vibronic energy levels $E_k\left(S_{12}, S_{34}\right)$ of the working cell and the corresponding spin-vibronic wave-functions

$$\left|k,S_{12}M_{12},S_{34}M_{34}\right\rangle=\sum_n\left[c_{13,n}^{k,S_{12},S_{34}}\left|(1,3)S_{12}M_{12},S_{34}M_{34}\right\rangle\left|n\right\rangle+c_{24,n}^{k,S_{12},S_{34}}\left|(2,4)S_{12}M_{12},S_{34}M_{34}\right\rangle\left|n\right\rangle\right], \quad (31)$$

where k =1, 2…numerates the vibronic states with the same S_{12}, S_{34} in the order of increasing of their energies. In the numerical diagonalization the size of the truncated vibronic matrix (maximal number n) is chosen to ensure reasonable accuracy of convergence.

Figure 7 shows a series of patterns of the low-lying spin-vibronic levels of isolated bi-dimeric square cell composed of d^1-d^2 (or d^8-d^9) dimers calculated as functions of vibronic coupling parameter υ for six different values of the ratio $\tau/|J|$. For PKS vibrational quantum in these calculations we use the value $\hbar\omega = 300\ \mathrm{cm}^{-1}$. For $\upsilon = 0$ the low-lying levels form the pure

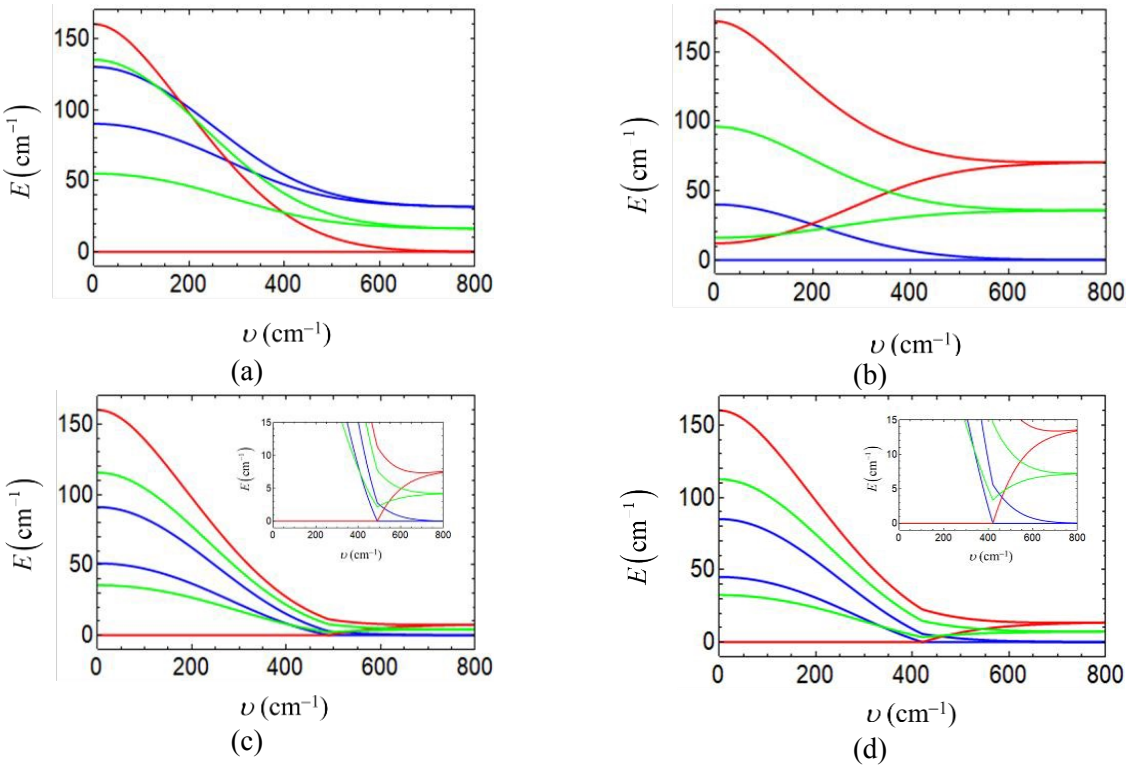

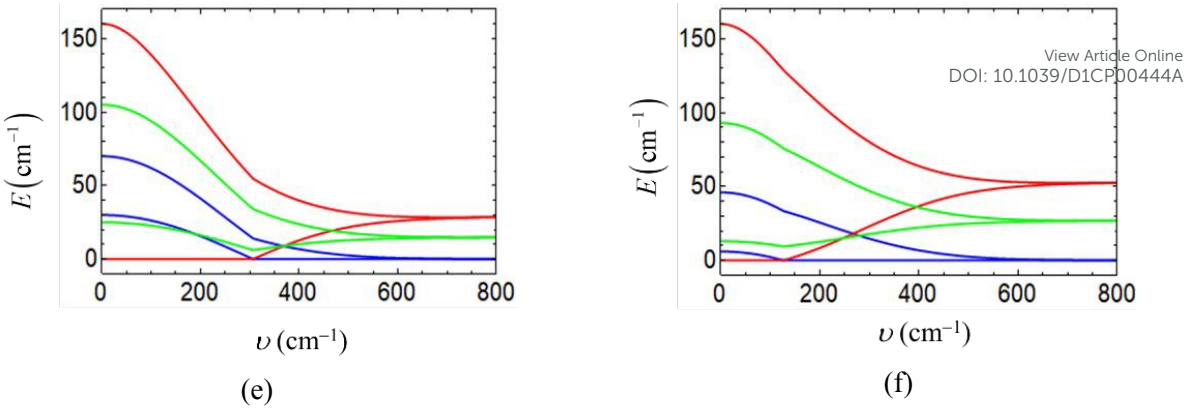

Fig. 7. Patterns of the spin-vibronic levels of isolated bi-dimeric square cell composed of d^1-d^2 (or d^8-d^9) dimers calculated as functions of vibronic coupling parameter υ with $\hbar\omega = 300\ \text{cm}^{-1}$, $\tau = 40\ \text{cm}^{-1}$ and $J = -5\ \text{cm}^{-1}$ (a), $-22\ \text{cm}^{-1}$ (b), $-11.5\ \text{cm}^{-1}$ (c), $-12.5\ \text{cm}^{-1}$ (d), $-15\ \text{cm}^{-1}$ (e), $-19\ \text{cm}^{-1}$ (f). Inserts in (c) and (d) show low-lying vibronic levels in the vicinity of critical value of υ at which the ground state changes its spin. The same coloring as in Fig. 5 is used. Only two lowest spin-vibronic levels for each set of S_{12}, S_{34} are shown.

electronic energy levels, which are obtained from Eq. (16) upon setting $P_2 = 0$. The increase of υ tends to suppress the electron delocalization and hence to decrease the resonance gaps between the lower and upper levels with the same set of S_{12}, S_{34}, which arise from the off-diagonal second-order DE. When the vibronic coupling is relatively strong and the lowest sheet of the adiabatic potential possesses deep minima, each such gap is reduced to the weak tunnel splitting of the lowest vibrational levels in the adiabatic potential minima. Finally, in the limit on strong vibronic coupling this splitting proves to be fully suppressed and the two levels become degenerate with respect to two diagonal distributions of the electronic pair. Such degenerate levels correspond to the two energetically equivalent adiabatic potential minima whose spin-dependence is described by Eq. (30).

It is seen from Fig. 7a that for $\tau/|J| < 2$ the ground state of the free cell has minimal dimeric spin values independently of the strength of the vibronic coupling. Figure 7b evidences that for $\tau/|J| > 4$ the ground state is also independent of υ but in this case it has maximal dimeric spin values. Figures 7 c-f confirm the fact that for $2 < \tau/|J| < 4$ the ground spin-state depends on the strength of the vibronic coupling, namely this state possesses maximal spin values $S_{12} = S_{34} = 3/2$ for weak vibronic coupling and minimal spin values $S_{12} = S_{34} = 1/2$ when this coupling is strong, with the critical value of υ being smaller for smaller ratio $\tau/|J|$ (compare Figs. 7c, 7d, 7e and 7f). The latter is because the electronic energy gap between the high-spin and low-spin states is

View Article Online
DOI: 10.1039/D1CP00444A

lower for smaller $\tau/|J|$ and hence weaker vibronic coupling is required to overcome this gap and to stabilize the state with $S_{12} = S_{34} = 1/2$.

11. Effect of the vibronic coupling on the field-induced spin switching and cell-cell response

The effect of the vibronic coupling on the field dependences of the energies of the spin-states can be realized by comparing such dependences evaluated in the framework of pure electronic model (left part in Fig. 6) with those calculated within the vibronic approach for υ = 400 cm^{-1} (central part in Fig. 6). Also, we will compare the cell-cell response functions evaluated for $\upsilon = 0$ (already discussed dependences shown by solid lines in the right part of Fig. 6) with those calculated for $\upsilon = 400$ cm^{-1} (dashed lines in the right part of Fig. 6).

In conformity with what has been found above, for $\tau/|J| > 4$ and for $\tau/|J| < 2$ the ground spin-state depends neither on the strength of the electrostatic field nor on the strength of the vibronic coupling. This is confirmed by Figs. 6a and 6b (central part), from which it is seen that at υ = 400 cm^{-1} the ground state has $S_{12} = S_{34} = 3/2$ for $\tau/|J| > 4$ and $S_{12} = S_{34} = 1/2$ for $\tau/|J| < 2$ independently of P_2, exactly as in the case of zero vibronic coupling (Figs. 6a and 6b, left part). At the same time, the vibronic coupling produces constructive effect on the cell-cell response function tending to enhance its nonlinearity and hence to improve the functional performance of QCA, as can be seen by comparing $P_1(P_2)$ dependences calculated for the cases of $\upsilon = 0$ and 400 cm^{-1} (see Figs. 6a and 6b, right part).

For $2 < \tau/|J| < 4$ (Figs. 6c-6f) the ground spin-state is determined both by the quadrupole field and by the vibronic coupling. Note that both these interactions produce similar effects on the ground state and the electric polarization of the cell since they both tend to localize the electronic pair. For this reason, at stronger vibronic coupling the effect of the quadrupole field becomes more pronounced affecting thus the spin-switching conditions. Considering, for example, the case of relatively weak HDVV exchange, one can see that at υ = 400 cm^{-1} the spin-switching occurs already at relatively weak quadrupole field (Fig. 6c, central part), while at $\upsilon = 0$ such switching proves to be impossible even provided that the driver-cell is fully polarized (Fig. 6c, left part) as has been discussed in Section 5. This leads to the drastic difference of the cell-cell response functions calculated for $\upsilon = 0$ and $\upsilon = 400$ cm^{-1} (Fig. 6c, right part). Indeed, the cell-cell response function for $\upsilon = 0$ proves to be monotonic, while for $\upsilon = 400$ cm^{-1} it exhibits discontinuous change at the critical field causing the spin-switching. For smaller ratio $\tau/|J|$ (Fig. 6d) the calculation predicts the spin-switching for both $\upsilon = 0$ and $\upsilon = 400$ cm^{-1}, but at $\upsilon = 400$ cm^{-1} the critical field able to induce the spin-switching proves to be much weaker than that at υ = 0 and hence

discontinuous change of P_1 also occurs at much smaller $|P_2|$ value. Finally, when the ratio $\tau/|J|$ only slightly exceeds 2 the vibronic coupling with $\upsilon = 400$ cm^{-1} is able to stabilize the state with minimal dimeric spins even at zero field. For this reason, no spin switching is possible in such case (Figs. 6e, 6f, central part) and so the cell-cell response function proves to be monotonic and strongly nonlinear (Figs 6e, 6f, right part, dashed line), which seems to be favorable for proper functioning of QCA based devices. In contrast, for $\upsilon = 0$ the ground state at $P_2 = 0$ is found to possesses maximal dimeric spins, which is able to change to the ground state with minimal dimeric spins under the action of the electrostatic field (Figs. 6e, 6f, left part) giving rise to the nonmonotonic behavior of the cell-cell response (Figs 6e, 6f, right part, solid line).

12. Concluding remarks

Herein we have examined a possibility to use multielectron MV dimers exhibiting DE and HDVV exchange to build the QCA cells and elucidated how the functional properties of the cells depend on the key intradimer and interdimer interactions, such as Coulomb repulsion, DE, HDVV exchange and vibronic coupling.

We have shown that in a definite parametric regime the square cells composed of the two $\mathrm{d}^n - \mathrm{d}^{n+1}$ - dimers exhibit monotonic nonlinear cell-cell response that means that they behave similarly to the conventional charge-transfer cells in which excess electrons are delocalized over the spinless cores. In other cases, the spin degrees of freedom have been shown to be of crucial importance in the sense that the electrostatic field created by the driver-cell not only polarize the excess electrons of the working cell but also causes the spin-switching accompanied by discontinuous change of the cell polarization. This finding inspires hope that the use of MV clusters exhibiting DE is promising for the design of multifunctional devices combining the properties of QCA with additional useful function of spin-switching that is accompanied with the conventional transformation of the charge configuration.

The proposed extension of the class of systems suitable for the creations of QCA devices includes both the arrays of multielectron paramagnetic quantum dots and the molecular MV clusters. As to the first kind of systems, it should be emphasized that engineering and manipulation with magnetic quantum dots is a successfully developing field combining fundamental and technological issues. As to the search for MV molecules acting as cells, it is a long-standing task although many fruitful efforts in this area have been applied. Regarding the magnetic dimers, they should not only contain spin cores required for the existence of DE, but also should possess the necessary chemical characteristics allowing such molecules to be attached to the surface. Still the existence of a large number of magnetic MV dimers exhibiting DE creates a hope that the use of such clusters as building blocks to design molecular cells for QCA could be a quite promising

strategy. The aim of the present article was solely to propose a new class of relevant systems for the design of molecular and quantum dots - based cells and to reveal the role of different interactions in the key characteristics of such cells. The comprehensive analysis of electronic, vibronic and molecular structures of possible candidates, as well as their quantum-chemical study can be regarded as challenging tasks for future.

Acknowledgements

The work was performed with funding from the Ministry of Science and Higher Education of the Russian Federation (Grant No. 075-15-2020-779) using computing facilities of the Laboratory of Molecular Magnetic Nanomaterials established under the agreement between the Ministry of Science and Higher Education of the Russian Federation and the Institute of Problems of Chemical Physics, Chernogolovka (Agreement No. 14.W03.31.0001).

References

1. Orlov, A. O.; Amlani, I.; Bernstein, G. H.; Lent, C. S.; Snider, G. L. Realization of a Functional Cell for Quantum-Dot Cellular Automata. *Science* **1997**, 277, 928−930.
2. Hänninen, I., Takala, J. Binary adders on quantum-dot cellular automata. *J. Signal Process. Syst*. **2010**, 58, 87–103.
3. Zoka, S., Gholami, M. A novel rising Edge triggered resettable D flip-flop using five input majority gate. *Microprocessors Microsyst*. **2018**, 1, 327–335.
4. Zoka, S.; Gholami, M. A novel efficient full adder–subtractor in QCA nanotechnology. *Int. Nano Lett*. **2019**, 9, 51-54.
5. Lent, C. S.; Tougaw, P. D.; Porod, W.; Bernstein, G. H. Quantum Cellular Automata. *Nanotechnology* **1993**, 4, 49 −57.
6. Lent, C. S.; Tougaw, P.; Porod, W. Bistable saturation in coupled quantum dots for quantum cellular automata. *Appl. Phys. Lett*. **1993**, 62, 714-716.
7. Lent, C. S.; Tougaw, P. D. Lines of interacting quantum-dot cells: A binary wire. *J. Appl. Phys*. **1993**, 74, 6227-6233.
8. Tougaw, P. D.; Lent, C. S. Logical devices implemented using quantum cellular automata. *J. Appl. Phys*. **1994**, 75**,** 1818-1825.
9. Lent, C.S.; Tougaw, P. D. A device architecture for computing with quantum dots. *Proc. IEEE* **1997**, 85, 541 - 557.
10. Porod, W.; Lent, C. S.; Bernstein, G. H.; Orlov, A. O.; Amlani, I.; Snider, G. L.; Merz, J. L. Quantum-Dot Cellular Automata: Computing with Coupled Quantum Dots. *Int. J. Electronics* **1999**, 86, 549 - 590.

11. Tóth, G.; Lent, C. S. Quasiadiabatic switching for metal-island quantum-dot cellular automata. *J. Appl. Phys*. **1999**, 85, 2977-2984.
12. Tóth, G.; Lent, C. S. Quantum computing with quantum-dot cellular automata. *Phys. Rev. A*. **2001**, 63, 052315.
13. Lent, C. S. Bypassing the Transistor Paradigm. *Science* **2000**, 288, 1597−1599.
14. Hennessy, K.; Lent, C. S. Clocking of Molecular Quantum-Dot Cellular Automata. *J. Vac. Sci. Technol., B: Microelectron. Process. Phenom*. **2001**, 19, 1752−1755.
15. Hush, N. Molecular Electronics: Cool Computing. *Nat. Mater*. **2003**, 2, 134−135.
16. Lent, C. S.; Isaksen, B.; Lieberman, M. Molecular Quantum-Dot Cellular Automata. *J. Am. Chem. Soc*. **2003**, 125, 1056−1063.
17. Jiao, J.; Long, G. J.; Grandjean, F.; Beatty, A. M.; Fehlner, T. P. Building Blocks for the Molecular Expression of Quantum Cellular Automata. Isolation and Characterization of a Covalently Bonded Square Array of Two Ferrocenium and Two Ferrocene Complexes. *J. Am. Chem. Soc.* **2003**, 125, 7522−7523.
18. Li, Z.; Beatty, A. M.; Fehlner, T. P. Molecular QCA Cells. 1. Structure and Functionalization of an Unsymmetrical Dinuclear Mixed-Valence Complex for Surface Binding. *Inorg. Chem*. **2003**, 42, 5707−5714.
19. Li, Z.; Fehlner, T. P. Molecular QCA Cells. 2. Characterization of an Unsymmetrical Dinuclear Mixed-Valence Complex Bound to a Au Surface by an Organic Linker. *Inorg. Chem*. **2003**, 42, 5715−5721.
20. Qi, H.; Sharma, S.; Li, Z.; Snider, G. L.; Orlov, A. O.; Lent, C. S.; Fehlner, T. P. Molecular Quantum Cellular Automata Cells. Electric Field Driven Switching of a Silicon Surface Bound Array of Vertically Oriented Two-Dot Molecular Quantum Cellular Automata. *J. Am. Chem. Soc*. **2003**, 125, 15250−15259.
21. Braun-Sand, S. B.; Wiest, O. Theoretical Studies of Mixed Valence Transition Metal Complexes for Molecular Computing. *J. Phys. Chem. A* **2003**, 107, 285−291.
22. Braun-Sand, S. B.; Wiest, O. Biasing Mixed-Valence Transition Metal Complexes in Search of Bistable Complexes for Molecular Computing. *J. Phys. Chem. B* **2003**, 107, 9624−9628.
23. Qi, H.; Gupta, A.; Noll, B. C.; Snider, G. L.; Lu, Y.; Lent, C.; Fehlner, T. P. Dependence of Field Switched Ordered Arrays of Dinuclear Mixed-Valence Complexes on the Distance between the Redox Centers and the Size of the Counterions. *J. Am. Chem. Soc*. **2005**, 127, 15218−15227.

24. Jiao, J.; Long, G. J.; Rebbouh, L.; Grandjean, F.; Beatty, A. M.; Fehlner, T. P. Properties of a Mixed-Valence $(Fe^{II})_2(Fe^{III})_2$ Square Cell for Utilization in the Quantum Cellular Automata Paradigm for Molecular Electronics. *J. Am. Chem. Soc*. **2005**, 127, 17819−17831.

25. Lu, Y.; Lent, C. S. Theoretical Study of Molecular Quantum Dot Cellular Automata. *J. Comput. Electron*. **2005**, 4, 115−118.

26. Zhao, Y.; Guo, D.; Liu, Y.; He, C.; Duan, C. A Mixed-Valence $(Fe^{II})_2(Fe^{III})_2$ Square for Molecular Expression of Quantum Cellular Automata. *Chem. Commun*. **2008**, 5725−5727.

27. Nemykin, V. N.; Rohde, G. T.; Barrett, C. D.; Hadt, R. G.; Bizzarri, C.; Galloni, P.; Floris, B.; Nowik, I.; Herber, R. H.; Marrani, A. G.; et al. Electron-Transfer Processes in Metal-Free Tetraferrocenylporphyrin. Understanding Internal Interactions to Access Mixed Valence States Potentially Useful for Quantum Cellular Automata. *J. Am. Chem. Soc*. **2009**, 131, 14969−14978.

28. Wang, X.; Yu, L.; Inakollu, V. S. S.; Pan, X.; Ma, J.; Yu, H. Molecular Quantum-Dot Cellular Automata Based on Diboryl Radical Anions. *J. Phys. Chem. C* **2018**, 122, 2454−2460.

29. Burgun, A.; Gendron, F.; Schauer, P. A.; Skelton, B. W.; Low, P. J.; Costuas, K.; Halet, J.-F.; Bruce, M. I.; Lapinte, C. Straightforward Access to Tetrametallic Complexes with a Square Array by Oxidative Dimerization of Organometallic Wires. *Organometallics* **2013**, 32, 5015−5025.

30. Schneider, B.; Demeshko, S.; Neudeck, S.; Dechert, S.; Meyer, F. Mixed-Spin [2 × 2] Fe_4 Grid Complex Optimized for Quantum Cellular Automata. *Inorg. Chem*. **2013**, 52, 13230−13237.

31. Christie, J. A.; Forrest, R. P.; Corcelli, S. A.; Wasio, N. A.; Quardokus, R. C.; Brown, R.; Kandel, S. A.; Lu, Y.; Lent, C. S.; Henderson, K. W. Synthesis of a Neutral Mixed-Valence Diferrocenyl Carborane for Molecular Quantum-Dot Cellular Automata Applications. *Angew. Chem., Int. Ed*. **2015**, 54, 15448−15671.

32. R. Makhoul, P. Hamon, T. Roisnel, J.-R. Hamon, C. Lapinte, A Tetrairon Dication Featuring Tetraethynylbenzene Bridging Ligand: A Molecular Prototype of Quantum Dot Cellular Automata, *Chem. Eur. J.* **2020**, 26, 8368 – 8371.

33. E. Rahimia , J. R. Reimers, Molecular quantum cellular automata cell design trade-offs: latching vs. power dissipation, *Phys. Chem. Chem. Phys.,* **2018**, 20, 17881-17888.

34. Y. Ardesi , A. Pulimeno, M. Graziano, F. Riente, G. Piccinini , Effectiveness of Molecules for Quantum Cellular Automata as Computing Devices, *J. Low Power Electron. Appl*. **2018**, 8, 24-43; doi:10.3390/jlpea8030024

35. Tsukerblat, B.; Palii, A.; Rybakov, A. Quantum cellular automata: theoretical study of

bistable cells for molecular computing. *Magn. Res. Solids* **2019**, 21, 19414.

36. Palii, A.; Zilberg, S.; Rybakov, A.; Tsukerblat, B. Double-Dimeric Versus Tetrameric Cells for Quantum Cellular Automata: a Semiempirical Approach to Evaluation of Cell−Cell Responses Combined with Quantum-Chemical Modeling of Molecular Structures, *J. Phys. Chem. C* **2019**, 123, 22614−22623.
37. Palii, A.; Clemente-Juan, J. M.; Rybakov, A.; Aldoshin, S.; Tsukerblat, B.; Exploration of the DE in quantum cellular automata: proposal for a new class of cells. *Chem. Commun.* **2020**, 56, 10682-10685.
38. Palii, A.; Clemente-Juan, J. M.; Aldoshin, S.; Korchagin, D.; Rybakov, A.; Zilberg, S.; Tsukerblat, S. Mixed-Valence Magnetic Molecular Cell for Quantum Cellular Automata: Prospects of Designing Multifunctional Devices through Exploration of Double Exchange. *J. Phys. Chem. C* **2020**, 124, 25602–25614.
39. Malinowski, F. K.; Martins, F.; Smith, T. B.; Bartlett, S. D.; Doherty, A. C.; Nissen, P. D. Spin of a Multielectron Quantum Dot and Its Interaction with a Neighboring Electron. *Phys. Rev. X* **2018**, 8, 011045.
40. Beaulac, R.; Archer, P. I.; Ochsenbein, S. T.; Gamelin, D. R. Mn^{2+}-Doped CdSe Quantum Dots: New Inorganic Materials for Spin-Electronics and Spin-Photonics. *Adv. Funct. Mater*. **2008**, 18, 3873–3891.
41. Schwartz, D. A.; Norberg, N. S.; Nguyen, Q. P.; Parker, J. M.; Gamelin, D. R. Magnetic Quantum Dots: Synthesis, Spectroscopy, and Magnetism of Co^{2+}- and Ni^{2+}-Doped ZnO Nanocrystals, *J. Am. Chem. Soc*. **2003**, 125, 13205–13218.
42. Drüeke, S.; Chaudhuri, P.; Pohl, K.; Wieghardt, K.; Ding, X.-Q.; Bill, E.; Sawaryn, A.; Trautwein, A. X.; Winkler, H.; Gurman, S. J. The Novel Mixed-valence, Exchange-coupled, Class III Dimer $[L_2Fe_2(\mu\text{-}OH)_3]^{2+}$ (L = N, N', N''-Trirnethyl-l ,4,7-triazacyclononane). *Chem. Commun*. **1989**, 59-62.
43. Mixed Valency Systems: Applications in Chemistry, Physics and Biology, Proceedings of the NATO Advanced Workshop on Mixed Valency Compounds held at Aghia Pelaghia, Crete, Greece, June 10-16, **1990**, Editor Prassides, K. NATO ASI Series, vol. 343 (D. Reidel Pub. Company, Dordrecht, Boston, London).
44. Blondin, G.; Girerd, J.-J. Interplay of Electron Exchange and Electron Transfer in Metal Polynuclear Complexes in Proteins or Chemical Models. *Chem. Rev*. **1990**, 90, 1359-1376.
45. Gamelin, D. R.; Bominaar, E. L.; Kirk, M. L.; Wieghardt, K; Solomon, E. I. Excited-State Contributions to Ground-State Properties of Mixed-Valence Dimers: Spectral and Electronic-Structural Studies of $[Fe_2(OH)_3(tmtacn)_2]^{2+}$ Related to the $[Fe_2S_2]$+ Active Sites of Plant-Type Ferredoxins. *J. Am. Chem. Soc.* **1996,** 118*,* 8085-8097.

46. Dutta, S. K.; Ensling, J.; Werner, R.; Florke, U.; Haase, W.; Giitlich, P.; Nag, K. Valence-Delocalized and Valence-Trapped Fe"Fe"' Complexes: Drastic Influence of the Ligands. Angen Chem. Inr. Ed. Engl. **1997**, 36,152-155.
47. Borras-Almenar, J. J.; Clemente-Juan, J. M.; Coronado, E.; Palii, A. V.; Tsukerblat, B. S. Magnetic Properties of Mixed-Valence Clusters: Theoretical Approaches and Applications. Magnetoscience: From Molecules to Materials, eds. Miller, J. Drillon, M. Villey-VCH, **2001**, 155-210.
48. Bechlars, B.; D'Alessandro, D. M.; Jenkins, D. M.; Iavarone, A. T.; Glover, S. D.; Kubiak, C. P.; Long, J. R. High-spin ground states via electron delocalization in mixed-valence imidazolate-bridged divanadium complexes. *Nat. Chem*. **2010**, 2, 362−368.
49. Gaudette, A. I.; Jeon, I.-R.; Anderson, J. S.; Grandjean, F.; Long, G. J.; Harris, T. D. Electron Hopping through Double-Exchange Coupling in a Mixed-Valence Diiminobenzoquinone-Bridged Fe_2 Complex. *J. Am. Chem. Soc.* **2015**, 137, 12617-12626.
50. Zener, C. Interaction between the d-Shells in the Transition Metals. II. Ferromagnetic Compounds of Manganese with Perovskite Structure. *Phys. Rev*. **1951**, 82, 403-405.
51. Anderson, P. W.; Hasegawa, H. Consideration of Double Exchange, *Phys. Rev*. **1955**, 100, 675-681.
52. De Gennes, P.-G. Effects of Double Exchange in Magnetic Crystals, *Phys. Rev*. **1960**, 118, 141-154.
53. J.-J. Girerd, V. Papaefthymiou, K. K. Surerus, E. Munck, Double exchange in iron-sulfur clusters and a proposed spin-dependent transfer mechanism, *Pure Appl. Chem*. **1989**, 61, 805-816.
54. Bosch-Serrano, C.; Clemente-Juan, J. M.; Coronado, E.; Gaita-Ariño, A.; Palii, A.; Tsukerblat, B. Molecular Analog of Multiferroics: Electric and Magnetic Field Effects in Many-Electron Mixed-Valence Dimers. *Phys. Rev. B* **2012**, 86, 024432.
55. Palii, A.; Clemente-Juan, J. M.; Tsukerblat, B.; Coronado, E. Electric field control of the optical properties in magnetic mixed valence molecules. *Chem. Sci*. **2014**, 5, 3598-3602.
56. Palii, A.; Aldoshin, S.; Tsukerblat, B. Mixed-valence clusters: Prospects for single-molecule magnetoelectrics. *Coord. Chem. Rev*. **2021**, 426, 213555.
57. Houck, S. E.; Mayhall, N. J. A Combined Spin-Flip and IP/EA Approach for Handling Spin and Spatial Degeneracies: Application to Double Exchange Systems. *J. Chem. Theory Comput*. **2019**, 15, 2278−2290.
58. Borras-Almenar, J. J.; Clemente-Juan, J. M.; Coronado, E.; Palii, A. V.; Tsukerblat, B. S. Anisotropic Double Exchange in Orbitally Degenerate Mixed Valence Systems. *Chem. Phys*. **2000**, 254, 275-285.

DOI: 10.1039/D1CP00444A

59. Palii, A. V. Double Exchange in a Pair of Transition Metal Ions with Unquenched Orbital Angular Momenta. *Phys. Lett. A* **2002**, 295, 147-153.

60. Tsukerblat, B.; Palii, A.; Clemente-Juan, J. M. Self-Trapping of Charge Polarized States in Four-Dot Molecular Quantum Cellular Automata: Bi-Electronic Tetrameric Mixed-Valence Species. *Pure Appl. Chem*. **2015**, 87, 271-282.

61. Tsukerblat, B.; Palii, A.; Clemente-Juan, J. M.; Coronado, E. Mixed-Valence Molecular Four-Dot Unit for Quantum Cellular Automata: Vibronic Self-Trapping and Cell-Cell Response. *J. Chem. Phys*. **2015**, 143, 134307.

62. Clemente-Juan, J. M.; Palii, A.; Coronado, E.; Tsukerblat, B. Mixed-Valence Molecular Unit for Quantum Cellular Automata: Beyond the Born-Oppenheimer Paradigm through the Symmetry Assisted Vibronic Approach. *J. Chem. Theory Comput*. **2016**, 12, 3545-3560.

63. Palii, A.; Tsukerblat, B.; Clemente-Juan, J. M.; Coronado, E. Spin Switching in Molecular Quantum Cellular Automata Based on Mixed-Valence Tetrameric Units. *J. Phys. Chem. C* **2016**, 120, 16994-17005.

64. Palii, A.; Tsukerblat, B. Tuning of Quantum Entanglement in Molecular Quantum Cellular Automata Based on Mixed-Valence Tetrameric Units. *Dalton Trans*. **2016**, 45, 16661-16672.

65. Palii, A.; Rybakov, A.; Aldoshin, S.; Tsukerblat, B. Semiclassical *versus* quantum-mechanical vibronic approach in the analysis of the functional characteristics of molecular quantum cellular automata. *Phys. Chem. Chem. Phys.* **2019**, 21, 16751-16761.

66. Piepho, S. B.; Krausz, E. R.; Schatz, P. N. Vibronic Coupling Model for Calculation of Mixed Valence Absorption Profiles. *J. Am. Chem. Soc*. **1978**, 100, 2996−3005.